

Supplementary Materials: Effects of Halide Ions on the Carbamidocyclophane Biosynthesis in *Nostoc* sp. CAVN2

Michael Preisitsch, Stefan E. Heiden, Monika Beerbaum, Timo H. J. Niedermeyer, Marie Schneefeld, Jennifer Herrmann, Jana Kumpfmüller, Andrea Thürmer, Inga Neidhardt, Christoph Wiesner, Rolf Daniel, Rolf Müller, Franz-Christoph Bange, Peter Schmieder, Thomas Schweder and Sabine Mundt

Table S1. Composition of Z½ medium used in this study.

Ingredient	mg/L H ₂ O
<i>Macronutrients</i> ^a	
NaNO ₃	233.5
Ca(NO ₃) ₂ ·4H ₂ O	29.5
K ₂ HPO ₄	15.5
MgSO ₄ ·7H ₂ O	12.5
Na ₂ CO ₃	10.6
<i>Micronutrients</i> ^b	
H ₃ BO ₃	0.24800
MnSO ₄ ·4H ₂ O	0.17840
KBr	0.00952
KI	0.00664
ZnSO ₄ ·7H ₂ O	0.02296
(NH ₄) ₆ Mo ₇ O ₂₄ ·4H ₂ O	0.00704
Na ₂ WO ₄ ·2H ₂ O	0.00264
KCr(SO ₄) ₂ ·12H ₂ O	0.00400
AlK(SO ₄) ₂ ·12H ₂ O	0.07584
Cd(NO ₃) ₂ ·4H ₂ O	0.01232
Co(NO ₃) ₂ ·6H ₂ O	0.01168
CuSO ₄	0.00640
NiSO ₄ ·7H ₂ O	0.01128
NH ₄ VO ₃	0.00184
<i>Other Components</i> ^c	
FeSO ₄ ·7H ₂ O	5.0
Na ₂ EDTA	20.0

^a Half quantity of macronutrients found in Zehnder-Medium according to Falch *et al.* [1]; ^b Micronutrient according to Gaffron's solution reported by Hughes *et al.* [2] in modified form; ^c Fe-EDTA-supplement according to Meffert *et al.* [3] in modified form.

Table S2. Biomass dry weights of *Nostoc* sp. CAVN2 cultures grown in the presence of different halogen salts at varying concentrations for 20–30 days. Values are presented as mean \pm standard error of the mean (SEM), $n = 2$.

CAVN2 Culture	Biomass Dry Weight (g/L)		
	20 Days	25 Days	30 Days
Control	0.39 \pm 0.03	0.40 \pm 0.05	0.47 \pm 0.00
+0.001% KF	0.40 \pm 0.02	0.46 \pm 0.02	0.50 \pm 0.02
+0.01% KF	0.42 \pm 0.01	0.42 \pm 0.04	0.50 \pm 0.04
+0.1% KF	0.28 \pm 0.03	0.33 \pm 0.03	0.39 \pm 0.03
+1.0% KF	0.17 \pm 0.01	0.20 \pm 0.02	0.23 \pm 0.02
+0.001% KI	0.36 \pm 0.00	0.39 \pm 0.01	0.44 \pm 0.05
+0.01% KI	0.36 \pm 0.03	0.43 \pm 0.04	0.43 \pm 0.03
+0.1% KI	0.20 \pm 0.00	0.25 \pm 0.02	0.38 \pm 0.11
+1.0% KI	0.17 \pm 0.03	0.15 \pm 0.05	0.19 \pm 0.05
+0.001% KBr	0.38 \pm 0.04	0.51 \pm 0.04	0.45 \pm 0.05
+0.01% KBr	0.36 \pm 0.02	0.46 \pm 0.05	0.51 \pm 0.01
+0.1% KBr	0.32 \pm 0.04	0.43 \pm 0.00	0.40 \pm 0.02
+1.0% KBr	0.44 \pm 0.03	0.47 \pm 0.02	0.48 \pm 0.07
+0.001% KCl	0.45 \pm 0.08	0.65 \pm 0.06	0.52 \pm 0.00
+0.01% KCl	0.41 \pm 0.04	0.49 \pm 0.11	0.54 \pm 0.06
+0.1% KCl	0.38 \pm 0.05	0.42 \pm 0.04	0.52 \pm 0.05
+1.0% KCl	0.50 \pm 0.05	0.54 \pm 0.01	0.63 \pm 0.00

Table S3. ¹H (600 MHz,) and ¹³C (150 MHz) NMR spectroscopic data for compounds 1–5 in MeOH-*d*₄ ^a.

No. ^b	1		2		3		4		5	
	δ_C , Type	δ_H (J in Hz)	δ_C , Type	δ_H (J in Hz)	δ_C , Type	δ_H (J in Hz)	δ_C , Type	δ_H (J in Hz)	δ_C , Type	δ_H (J in Hz)
1	84.9, CH	4.93, <i>d</i> (10.1)	84.9, CH	4.90, <i>d</i> (10.4)	84.9, CH	4.93, <i>d</i> (10.1)	84.6, CH	4.90, <i>d</i> (10.1)	84.8, CH	4.90, <i>d</i> (10.2)
2	41.7, CH	1.81, <i>m</i>	41.7, CH	1.81, <i>m</i>	41.8, CH	1.84, <i>m</i>	41.8, CH	1.81, <i>m</i>	41.7, CH	1.81, <i>m</i>
3	35.9, CH ₂	0.87, 0.79, <i>m</i>	36.0, CH ₂	0.87, 0.79, <i>m</i>	35.9, CH ₂	0.91, 0.82, <i>m</i>	35.8, CH ₂	0.87, 0.80, <i>m</i>	35.8, CH ₂	0.87, 0.80, <i>m</i>
4	31.0, CH ₂	1.52, n.o., <i>m</i>	31.0, CH ₂	1.52, n.o., <i>m</i>	31.0, CH ₂	1.56, 0.92, <i>m</i>	30.9, CH ₂	1.53, 0.92, <i>m</i>	30.9, CH ₂	1.53, 0.92, <i>m</i>
5	31.7, CH ₂	1.03, 0.81, <i>m</i>	31.8, CH ₂	1.04, 0.81, <i>m</i>	31.8, CH ₂	1.07, 0.84, <i>m</i>	31.8, CH ₂	1.05, 0.81, <i>m</i>	31.8, CH ₂	1.05, 0.81, <i>m</i>
6	36.6, CH ₂	2.12, 1.41, <i>m</i>	36.6, CH ₂	2.13, 1.41, <i>m</i>	36.6, CH ₂	2.15, 1.44, <i>m</i>	36.6, CH ₂	2.13, 1.42, <i>m</i>	36.6, CH ₂	2.13, 1.42, <i>m</i>
7	37.9, CH	3.27, <i>m</i>	37.9	3.27, <i>m</i>	37.7, CH	3.31, <i>m</i>	37.7, CH	3.28, <i>m</i>	37.7, CH	3.28, <i>m</i>
8	119.1, C		119.1, C		119.7, C		119.9, C		118.7, C	
9	158.4, C		160.2, C		160.2, C		161.2, C		160.2, C	
10	106.6, CH	6.28, <i>s</i>	106.6, CH	6.28, <i>s</i>	106.6, CH	6.24, <i>s</i>	106.8, CH	6.22, <i>s</i>	106.6, CH	6.22, <i>s</i>
11	141.2, C		141.3, C		141.4, C		141.8, C		141.5, C	
12	110.7, CH	6.21, <i>s</i>	110.7, CH	6.21, <i>s</i>	110.8, CH	6.31, <i>s</i>	110.8, CH	6.28, <i>s</i>	110.8, CH	6.28, <i>s</i>
13	158.4, C		158.5, C		158.4, C		158.3, C		158.4, C	
14	84.9, CH	4.93, <i>d</i> (10.1)	84.9, CH	4.90, <i>d</i> (10.4)	84.9, CH	4.93, <i>d</i> (10.1)	84.6, CH	4.90, <i>d</i> (10.1)	84.8, CH	4.90, <i>d</i> (10.2)
15	41.7, CH	1.81, <i>m</i>	41.7, CH	1.81, <i>m</i>	41.8, CH	1.84, <i>m</i>	41.8, CH	1.81, <i>m</i>	41.7, CH	1.81, <i>m</i>
16	35.9, CH ₂	0.87, 0.79, <i>m</i>	36.0, CH ₂	0.87, 0.79, <i>m</i>	35.9, CH ₂	0.91, 0.82, <i>m</i>	35.8, CH ₂	0.87, 0.80, <i>m</i>	35.8, CH ₂	0.87, 0.80, <i>m</i>
17	31.0, CH ₂	1.52, n.o., <i>m</i>	31.0, CH ₂	1.52, n.o., <i>m</i>	31.0, CH ₂	1.56, 0.92, <i>m</i>	30.9, CH ₂	1.53, 0.92, <i>m</i>	30.9, CH ₂	1.53, 0.92, <i>m</i>
18	31.7, CH ₂	1.03, 0.81, <i>m</i>	31.8, CH ₂	1.04, 0.81, <i>m</i>	31.8, CH ₂	1.07, 0.84, <i>m</i>	31.8, CH ₂	1.05, 0.81, <i>m</i>	31.8, CH ₂	1.05, 0.81, <i>m</i>
19	36.6, CH ₂	2.12, 1.41, <i>m</i>	36.6, CH ₂	2.13, 1.41, <i>m</i>	36.6, CH ₂	2.15, 1.44, <i>m</i>	36.6, CH ₂	2.13, 1.42, <i>m</i>	36.6, CH ₂	2.13, 1.42, <i>m</i>
20	38.1, CH	3.24, <i>m</i>	37.9	3.27, <i>m</i>	38.2, CH	3.27, <i>m</i>	37.7, CH	3.28, <i>m</i>	37.7, CH	3.28, <i>m</i>
21	119.7, C		119.1, C		118.7, C		119.9, C		118.7, C	
22	158.4, C		160.2, C		160.2, C		161.2, C		160.2, C	
23	106.6, CH	6.28, <i>s</i>	106.6, CH	6.28, <i>s</i>	106.6, CH	6.24, <i>s</i>	106.8, CH	6.22, <i>s</i>	106.6, CH	6.22, <i>s</i>
24	141.2, C		141.3, C		141.4, C		141.8, C		141.5, C	
25	110.7, CH	6.21, <i>s</i>	110.7, CH	6.21, <i>s</i>	110.8, CH	6.31, <i>s</i>	110.8, CH	6.28, <i>s</i>	110.8, CH	6.28, <i>s</i>
26	158.4, C		158.5, C		158.4, C		158.3, C		158.4, C	
27	35.4, CH ₂	2.06, 1.60, <i>m</i>		2.06, 1.59, <i>m</i>	34.7, CH ₂	2.14, 1.64, <i>m</i>	34.7, CH ₂	2.11, 1.61, <i>m</i>	34.7, CH ₂	2.11, 1.61, <i>m</i>
28	29.3, CH ₂	1.39, 1.32, <i>m</i>	29.3, CH ₂	1.39, 1.32, <i>m</i>	29.2, CH ₂	1.64, 1.49, <i>m</i>	29.2, CH ₂	1.61, 1.46, <i>m</i>	29.2, CH ₂	1.61, 1.46, <i>m</i>
29	35.8, CH ₂	1.90, 1.84, <i>m</i>	35.8, CH ₂	1.91, 1.83, <i>m</i>	48.3, CH ₂	2.50, 2.38, <i>m</i>	48.3, CH ₂	2.47, 2.35, <i>m</i>	48.3, CH ₂	2.47, 2.35, <i>m</i>
30	35.8, CH ₂	3.42, <i>td</i> (7.0, 0.9)	35.8, CH ₂	3.42, <i>td</i> (7.1, 0.8)	49.3, CH	5.91, <i>t</i> (6.3)	49.3, CH	5.88, <i>t</i> (6.4)	49.3, CH	5.88, <i>t</i> (6.3)

Table S3. Cont.

31	36.2, CH ₂	2.00, 1.58, <i>m</i>	35.4, CH ₂	2.06, 1.59, <i>m</i>	36.2, CH ₂	2.03, 1.61, <i>m</i>	35.4, CH ₂	2.06, 1.60, <i>m</i>	34.7, CH ₂	2.11, 1.61, <i>m</i>
32	33.0, CH ₂	1.29, 1.19, <i>m</i>	29.3, CH ₂	1.39, 1.32, <i>m</i>	33.0, CH ₂	1.29, 1.19, <i>m</i>	29.1, CH ₂	1.46, 1.33, <i>m</i>	29.2, CH ₂	1.61, 1.46, <i>m</i>
33	25.3, CH ₂	1.33, n.o., <i>m</i>	35.8, CH ₂	1.91, 1.83, <i>m</i>	25.3, CH ₂	1.40, 1.34, <i>m</i>	35.7, CH ₂	1.91, 1.84, <i>m</i>	48.3, CH ₂	2.47, 2.35, <i>m</i>
34	15.8, CH ₃	0.90, <i>t</i> (7.2)	35.8, CH ₂	3.42, <i>td</i> (7.1, 0.8)	15.9, CH ₃	0.93, <i>t</i> (7.2)	35.8, CH ₂	3.42, <i>td</i> (7.0, 1.2)	49.3, CH	5.88, <i>t</i> (6.3)
35	17.9, CH ₃	1.09, <i>d</i> (6.4)	17.9, CH ₃	1.09, <i>d</i> (6.4)	17.9, CH ₃	1.12, <i>d</i> (6.4)	17.9, CH ₃	1.09, <i>d</i> (6.4)	17.9, CH ₃	1.09, <i>d</i> (6.4)
36	17.9, CH ₃	1.09, <i>d</i> (6.4)	17.9, CH ₃	1.09, <i>d</i> (6.4)	17.9, CH ₃	1.12, <i>d</i> (6.4)	17.9, CH ₃	1.09, <i>d</i> (6.4)	17.9, CH ₃	1.09, <i>d</i> (6.4)
37	161.3, C		161.2, C		161.3, C		162.3, C		161.2, C	
38	161.3, C		161.2, C		161.3, C		162.3, C		161.2, C	

^a ¹³C chemical shifts obtained from HMQC and HMBC spectra; Abbreviation: n.o. = not observed; ^b Numbering of the carbamidocyclophane framework, see Figure 4A.

Table S4. ¹H (600 MHz) and ¹³C (150 MHz) NMR spectroscopic data for compounds 6–9 in MeOH-*d*₄. ^a

No. ^b	6		7		8		9	
	δ_C , Type	δ_H (J in Hz)	δ_C , Type	δ_H (J in Hz)	δ_C , Type	δ_H (J in Hz)	δ_C , Type	δ_H (J in Hz)
1	84.9, CH	4.93, <i>d</i> (10.4)	84.9, CH	4.90, <i>d</i> (10.3)	84.9, CH	4.90, <i>d</i> (10.6)	85.0, CH	4.89, <i>d</i> (10.4)
2	41.8, CH	1.85, <i>m</i>	41.8, CH	1.82, <i>m</i>	41.8, CH	1.82, <i>m</i>	41.7, CH	1.82, <i>m</i>
3	35.9, CH ₂	0.89, 0.79, <i>m</i>	35.9, CH ₂	0.88, 0.79, <i>m</i>	35.9, CH ₂	0.88, 0.80, <i>m</i>	35.9, CH ₂	0.88, 0.79, <i>m</i>
4	31.2, CH ₂	1.54, n.o., <i>m</i>	31.2, CH ₂	1.51, 0.91, <i>m</i>	31.1, CH ₂	1.51, 0.90, <i>m</i>	31.0, CH ₂	1.53, 0.90, <i>m</i>
5	31.9, CH ₂	1.03, 0.80, <i>m</i>	31.9, CH ₂	1.04, 0.80, <i>m</i>	31.8, CH ₂	1.03, 0.81, <i>m</i>	31.8, CH ₂	1.03, 0.81, <i>m</i>
6	36.8, CH ₂	2.15, 1.43, <i>m</i>	36.7, CH ₂	2.13, 1.41, <i>m</i>	36.7, CH ₂	2.13, 1.41, <i>m</i>	36.7, CH ₂	2.14, 1.41, <i>m</i>
7	37.9, CH	3.30, <i>m</i>	37.7, CH	3.28, <i>m</i>	37.8, CH	3.28, <i>m</i>	37.7, CH	3.28, <i>m</i>
8	119.2, 119.7, C		119.2, 119.7, C		119.2, 119.7, C		119.9, C	
9	160.3, C		160.3, C		160.2, C		160.3, C	
10	106.6, CH	6.32, <i>s</i>	106.7, CH	6.31, <i>s</i>	106.6, CH	6.30, <i>s</i>	106.9, CH	6.29, <i>s</i>
11	141.2, C		141.3, C		141.4, C		141.8, C	
12	110.8, CH	6.20, <i>s</i>	110.9, CH	6.24, <i>s</i>	110.8, CH	6.22, <i>s</i>	111.0, CH	6.22, <i>s</i>
13	158.4, C		158.4, C		158.4, C		n.o.	
14	83.1, CH	3.86, <i>d</i> (9.8)	83.1, CH	3.84, <i>d</i> (9.6)	83.1, CH	3.84, <i>d</i> (9.5)	83.2, CH	3.83, <i>d</i> (9.5)
15	43.4, CH	1.66, <i>m</i>	43.4, CH	1.63, <i>m</i>	43.4, CH	1.63, <i>m</i>	43.4, CH	1.63, <i>m</i>
16	36.6, CH ₂	0.85, 0.74, <i>m</i>	36.6, CH ₂	0.83, 0.72, <i>m</i>	36.5, CH ₂	0.82, 0.71, <i>m</i>	36.5, CH ₂	0.83, 0.73, <i>m</i>

Table S4. Cont.

17	31.2, CH ₂	1.54, n.o., <i>m</i>	31.2, CH ₂	1.51, 0.91, <i>m</i>	31.1, CH ₂	1.51, 0.91, <i>m</i>	31.1, CH ₂	1.51, n.o., <i>m</i>
18	31.9, CH ₂	1.03, 0.80, <i>m</i>	31.9, CH ₂	1.04, 0.80, <i>m</i>	31.8, CH ₂	1.03, 0.81, <i>m</i>	31.8, CH ₂	1.03, 0.81, <i>m</i>
19	36.8, CH ₂	2.15, 1.43, <i>m</i>	36.7, CH ₂	2.13, 1.41, <i>m</i>	36.7, CH ₂	2.13, 1.41, <i>m</i>	36.7, CH ₂	2.14, 1.41, <i>m</i>
20	38.2, CH	3.27, <i>m</i>	38.2, CH	3.24, <i>m</i>	37.8, CH	3.28, <i>m</i>	37.7, CH	3.28, <i>m</i>
21	118.5, 119.0, C		118.5, 119.0, C		118.5, 119.0, C		118.3, C	
22	160.2, C		160.4, C		160.3, C		160.3, C	
23	106.4, CH	6.18, <i>s</i>	106.5, CH	6.36, <i>s</i>	106.4, CH	6.34, <i>s</i>	106.6, CH	6.33, <i>s</i>
24	145.4, C		145.5, C		145.6, C		146.0, C	
25	110.2, CH	6.35, <i>s</i>	110.3, CH	6.19, <i>s</i>	110.2, CH	6.16, <i>s</i>	110.4, CH	6.16, <i>s</i>
26	158.4, C		158.5, C		158.4, C		n.o.	
27	35.4, CH ₂	2.11, 1.61, <i>m</i>	35.4, CH ₂	2.06, 1.59, <i>m</i>	34.8, CH ₂	2.13, 1.60, <i>m</i>	34.7, CH ₂	2.12, 1.60, <i>m</i>
28	29.2, CH ₂	1.38, 1.33, <i>m</i>	29.2, CH ₂	1.60, 1.45, <i>m</i>	29.2, CH ₂	1.60, 1.45, <i>m</i>	29.1, CH ₂	1.60, 1.45, <i>m</i>
29	35.8, CH ₂	1.93, n.o., <i>m</i>	48.3, CH ₂	2.49, 2.35, <i>m</i>	48.2, CH ₂	2.48, 2.34, <i>m</i>	48.3, CH ₂	2.48, 2.34, <i>m</i>
30	35.9, CH ₂	3.43, <i>m</i>	49.4, CH	5.89, <i>t</i> (6.3)	49.4, CH	5.89, <i>td</i> (6.3, 1.4)	49.3, CH	5.88, <i>td</i> (6.3, 1.4)
31	36.2, CH ₂	2.03, 1.59, <i>m</i>	36.2, CH ₂	2.01, 1.57, <i>m</i>	35.3, CH ₂	2.08, 1.59, <i>m</i>	34.7, CH ₂	2.12, 1.60, <i>m</i>
32	33.1, CH ₂	1.28, 1.17, <i>m</i>	33.2, CH ₂	1.26, 1.19, <i>m</i>	29.2, CH ₂	1.42, 1.35, <i>m</i>	29.1, CH ₂	1.60, 1.45, <i>m</i>
33	25.3, CH ₂	1.40, 1.32, <i>m</i>	25.3, CH ₂	1.37, 1.28, <i>m</i>	35.5, CH ₂	1.91, 1.84, <i>m</i>	48.3, CH ₂	2.48, 2.34, <i>m</i>
34	15.9, CH ₃	0.92, <i>m</i>	15.9, CH ₃	0.90, <i>m</i>	35.9, CH ₂	3.41, <i>m</i>	49.3, CH	5.88, <i>td</i> (6.3, 1.4)
35	18.0, CH ₃	1.12, <i>d</i> (6.1)	18.0, CH ₃	1.09, <i>d</i> (6.3)	17.9, CH ₃	1.09, <i>d</i> (6.4)	17.9, CH ₃	1.09, <i>d</i> (6.4)
36	18.3, CH ₃	1.17, <i>d</i> (6.1)	18.3, CH ₃	1.15, <i>d</i> (6.3)	18.3, CH ₃	1.14, <i>d</i> (6.4)	18.3, CH ₃	1.15, <i>d</i> (6.4)
37	161.3, C		161.3, C		161.2, C		161.5, C	

^a ¹³C chemical shifts obtained from HMQC and HMBC spectra; Abbreviation: n.o. = not observed; ^b Numbering of the carbamidocyclophane framework, see Figure 4A.

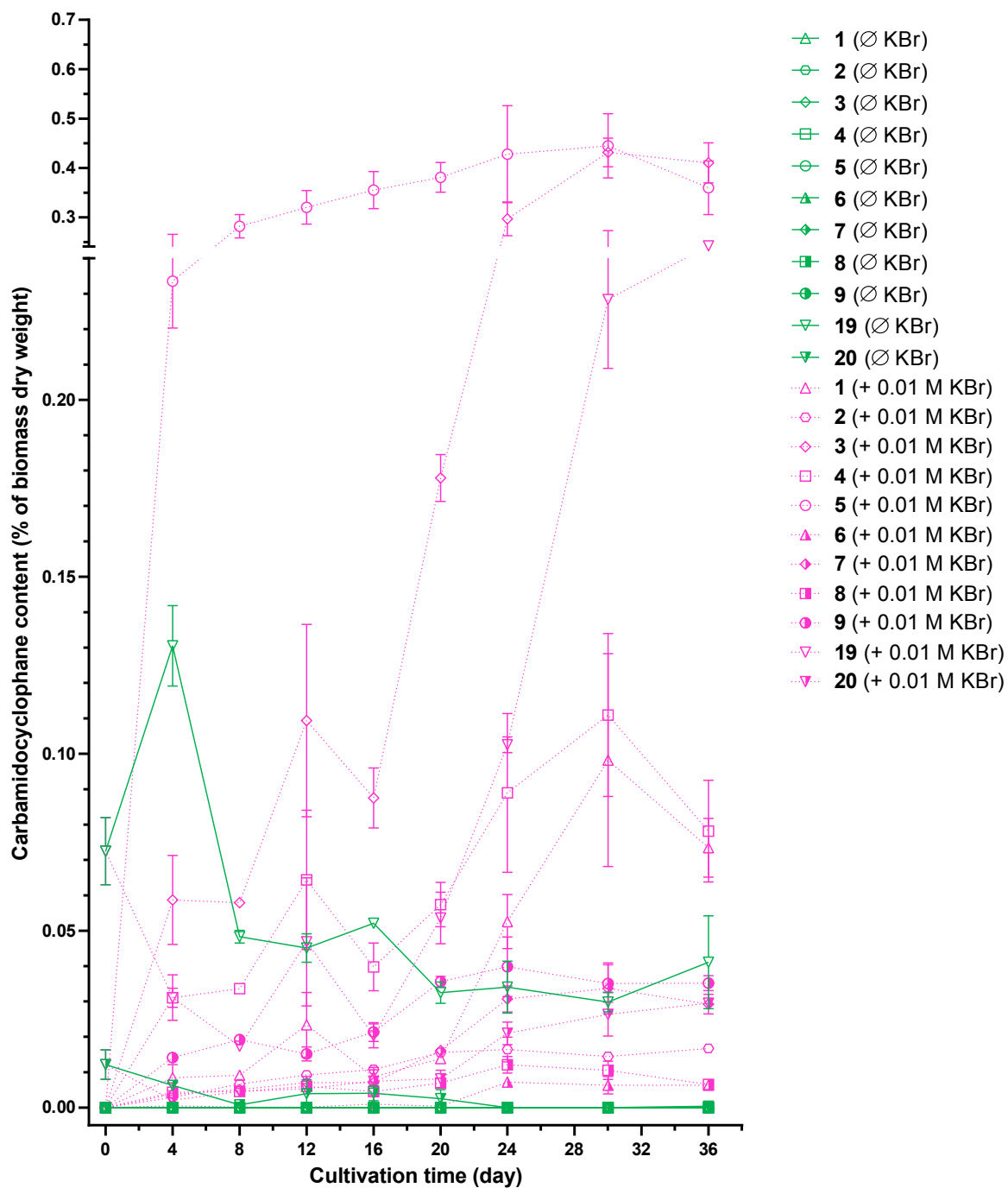


Figure S1. Intracellular contents of brominated (1–9) and non-halogenated (19 and 20) carbamidocyclophanes of *Nostoc* sp. CAVN2 cultivated in $Z\frac{1}{2}$ medium as control containing $<0.1 \mu\text{M}$ halide ions (\emptyset KBr) or in bromide-enriched (+0.01 M KBr) $Z\frac{1}{2}$ medium. Values shown are expressed as the mean \pm SEM, $n = 3$.

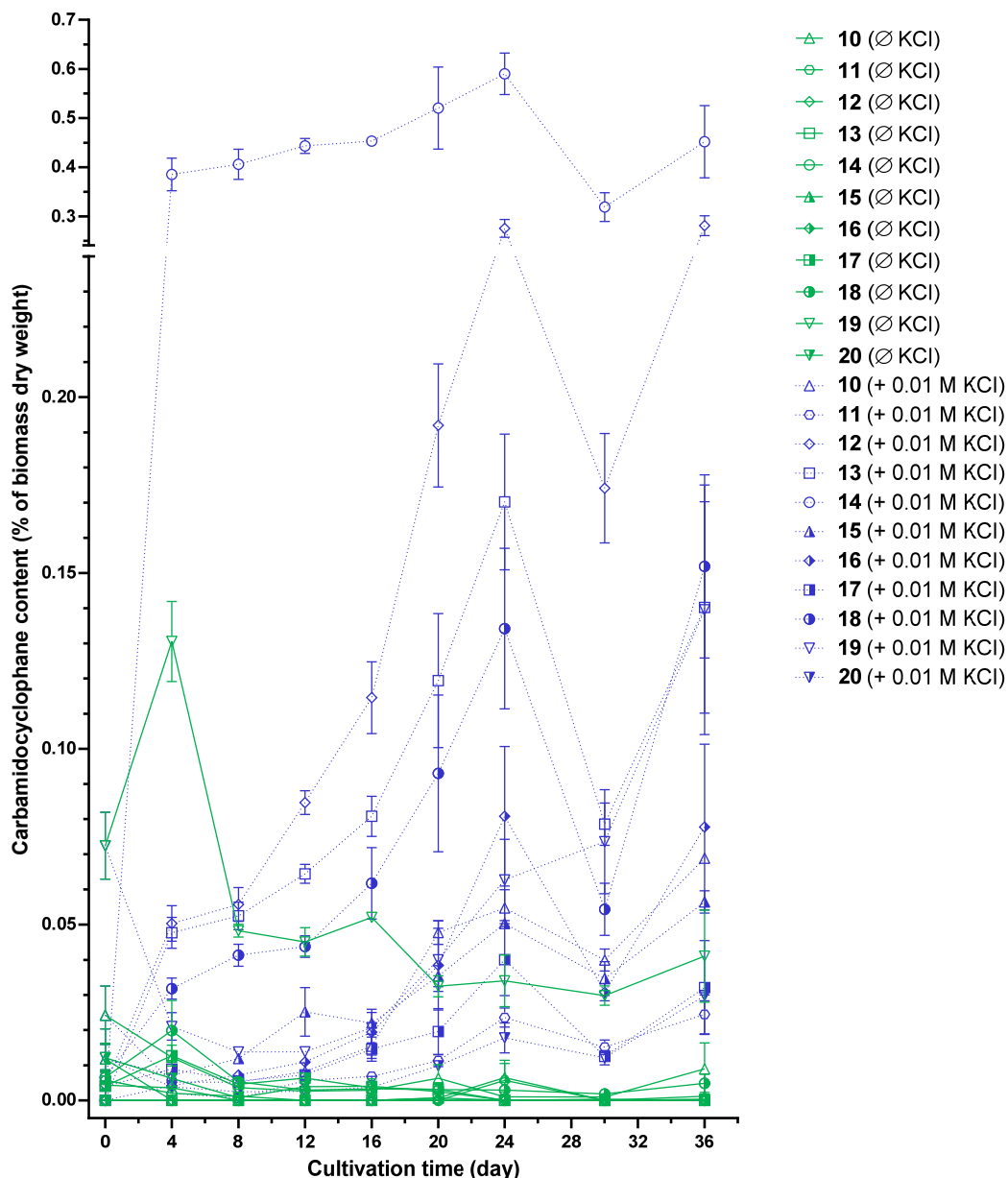


Figure S2. Intracellular contents of chlorinated (10–18) and non-halogenated (19 and 20) carbamidocyclophanes of *Nostoc* sp. CAVN2 cultivated in Z½ medium as control containing <math><0.1 \mu\text{M}</math> halide ions (Ø KCl) or in chloride-enriched (+ 0.01 M KCl) Z½ medium. Values shown are expressed as the mean \pm SEM, $n = 3$.

Table S5. Biomass dry weights of *Nostoc* sp. CAVN2 cultures grown in the presence of KCl and KBr at different mixing ratios for 20 days. Values are presented as mean \pm SEM, $n = 3$.

CAVN2 Culture	Biomass Dry Weight (g/L)	Statistical Significance versus the Control ^a
Control	0.35 \pm 0.01	
+0.01 M KCl and 0.01 M KBr	0.77 \pm 0.03	**
+0.01 M KCl and 0.001 M KBr	0.68 \pm 0.02	No
+0.001 M KCl and 0.01 M KBr	0.64 \pm 0.03	No

^a Two asterisks (**) indicate a significant difference of $p < 0.01$ versus the control; Data were tested for Gaussian distribution using the Kolmogorov-Smirnov test; Statistical analysis was performed using the Kruskal-Wallis test followed by Dunn's multiple comparisons test.

Table S6. List of predicted open reading frames (ORF) of the *cab* gene cluster. ^a

ORF	Annotation	Protein	Amino Acids	Top BlastP Result Protein [Organism] (Acc. No.)	Ident/Sim/Qcov (%), E-Value	InterPro Results
1	Caspase-like domain-containing protein		220	Hypothetical protein [<i>Scytonema hofmanni</i> UTEX B 1581] (WP_051502726)	56/68/87.27, 8.16e-57	Caspase-like domain(IPR029030)
2	Long-chain-fatty-acid – CoA ligase	CabA	604	AMP-dependent synthetase/ligase [<i>Cylindrospermum licheniforme</i> UTEX B 2014] (AFV96135)	88/94/99.83, 0	AMP-dependent synthetase/ligase (IPR000873)
3	Acyl carrier protein	CabB	103	Acyl carrier protein [<i>C. licheniforme</i> UTEX B 2014] (AFV96136)	87/90/100, 1.61e-57	Acyl carrier protein-like (IPR009081)
4	Hypothetical protein	CabC	471	Hypothetical protein [<i>C. licheniforme</i> UTEX B 2014] (AFV96137)	96/97/100, 0	None
5	Polyketide synthase	CabD	1,385	Polyketide synthase [<i>C. licheniforme</i> UTEX B 2014] (AFV96138)	88/94/77.11, 0	Polyketide synthase, beta-ketoacyl synthase domain (IPR020841), acyl transferase domain (IPR020801), 3× phosphopantetheine-binding domain (IPR020806)
6	Beta-ketoacyl synthase	CabE	413	Beta-ketoacyl synthase [<i>C. licheniforme</i> UTEX B 2014] (AFV96139)	92/96/100, 0	Polyketide synthase, beta-ketoacyl synthase domain (IPR020841)
7	Hydroxymethylglutaryl-CoA synthase	CabF	419	3-Hydroxy-3-methylglutaryl CoA synthase [<i>Cylindrospermum stagnale</i>] (WP_015207399)	94/98/100, 0	Hydroxymethylglutaryl-coenzyme A synthase, N-terminal (IPR013528), C-terminal domain (IPR013746)
8	Enoyl-CoA hydratase	CabG	258	Enoyl-CoA hydratase/isomerase [<i>C. licheniforme</i> UTEX B 2014] (AFV96141)	90/95/98.45, 1.41e-162	Crotonase superfamily (IPR001753)

Table S6. Cont.

9	Polyketide synthase	CabH	2077	Polyketide synthase family protein [<i>C. stagnale</i>] (WP_015207397)	84/91/68.85, 0	Crotonase superfamily (IPR001753); Polyketide synthase, enoylreductase domain (IPR020843), beta-ketoacyl synthase domain (IPR020841), acyl transferase domain (IPR020801), phosphopantetheine-binding domain (IPR020806); Thioesterase (IPR001031)
10	Type III polyketide synthase	CabI	373	Naringenin-chalcone synthase [<i>C. stagnale</i>] (WP_015207396)	92/97/100, 0	FAE1/Type III polyketide synthase-like protein (IPR013601); Chalcone/stilbene synthase, C-terminal (IPR012328)
11	Isoprenylcysteine carboxyl methyltransferase	CabJ	199	Phospholipid methyltransferase [<i>C. licheniforme</i> UTEX B 2014] (AFV96144)	84/94/100, 3.66e-122	Isoprenylcysteine carboxyl methyltransferase (IPR007269)
12	Beta-propeller repeat-containing protein	CabK	687	Hemolysin-type calcium-binding region [<i>C. licheniforme</i> UTEX B 2014] (AFV96145)	79/90/92.87, 0	Quinonprotein alcohol dehydrogenase- like superfamily (IPR011047); Beta-propeller repeat (IPR010620)
13	Carbamoyltransferase	CabL	581	Hypothetical protein [Methylococcaceae bacterium Sn10-6] (WP_052700247)	52/68/71.08, 6.74e-150	Carbamoyltransferase (IPR003696)
14	Rieske [2Fe-2S] iron-sulphur domain- containing protein	CabM	502	Ring-hydroxylating dioxygenase [<i>C. stagnale</i>] (WP_015207391)	89/95/100, 0	Rieske [2Fe-2S] iron-sulphur domain (IPR017941); Pheophorbide a oxygenase (IPR013626)

^a Abbreviations: Acc. No. = accession number; Ident = identity, Sim = similarity, Qcov = query coverage, E-value = expectation value.

Table S7. Results of the MegaBLAST search of the *C. licheniforme* UTEX 'B 2014' *cyl* gene cluster (query) against the *Nostoc* sp. CAVN2 *cab* gene cluster (subject).

Identity (%)	Alignment Length	Mismatches	Gap Opens	Query		Subject		E-Value	Bit Score
				Start	End	Start	End		
88.78	1880	206	4	1005	2879	1337	3216	0	2298.0
84.60	448	51	10	3345	3788	3275	3708	4e-121	429.0
91.08	4954	423	9	3924	8865	3833	8779	0	6682.0
85.01	467	68	2	8478	8943	8791	9256	2e-134	473.0
89.56	5767	573	19	8886	14646	9276	15019	0	7287.0
83.51	97	16	0	14691	14787	14923	15019	2e-19	91.6
76.68	223	36	7	14832	15054	14923	15129	5e-25	110.0
87.72	6148	687	40	15058	21189	15044	21139	0	7108.0
85.66	1980	273	10	21414	23388	21468	23441	0	2073.0

Table S8. Results of the MegaBLAST search of the *Nostoc* sp. CAVN2 *cab* gene cluster (query) against the *C. stagnale* PCC 7417 gene cluster (subject).

Identity (%)	Alignment Length	Mismatches	Gap Opens	Query		Subject		E-Value	Bit Score
				Start	End	Start	End		
88.46	1881	207	6	1337	3216	797	2668	0	2263.0
89.75	5979	565	25	3275	9223	2853	8813	0	7601.0
86.36	396	54	0	8384	8779	8372	8767	3e-122	433.0
85.27	387	57	0	8791	9177	7981	8367	3e-122	399.0
89.64	5744	565	20	9300	15019	8799	14536	0	7284.0
82.47	97	17	0	14923	15019	14581	14677	1e-17	86.1
83.51	97	16	0	14923	15019	14722	14818	2e-19	91.6
87.07	6282	726	43	14923	21139	14863	21123	0	7023.0
86.34	1999	264	8	21468	23461	21349	23343	0	2170.0
91.51	106	8	1	23775	23880	23650	23754	2e-35	145.0
95.31	128	6	0	23871	23998	24026	24153	3e-53	204.0
87.25	659	55	13	25853	26482	24185	24843	0	725.0
90.80	1630	135	4	26727	28341	25970	27599	0	2165.0

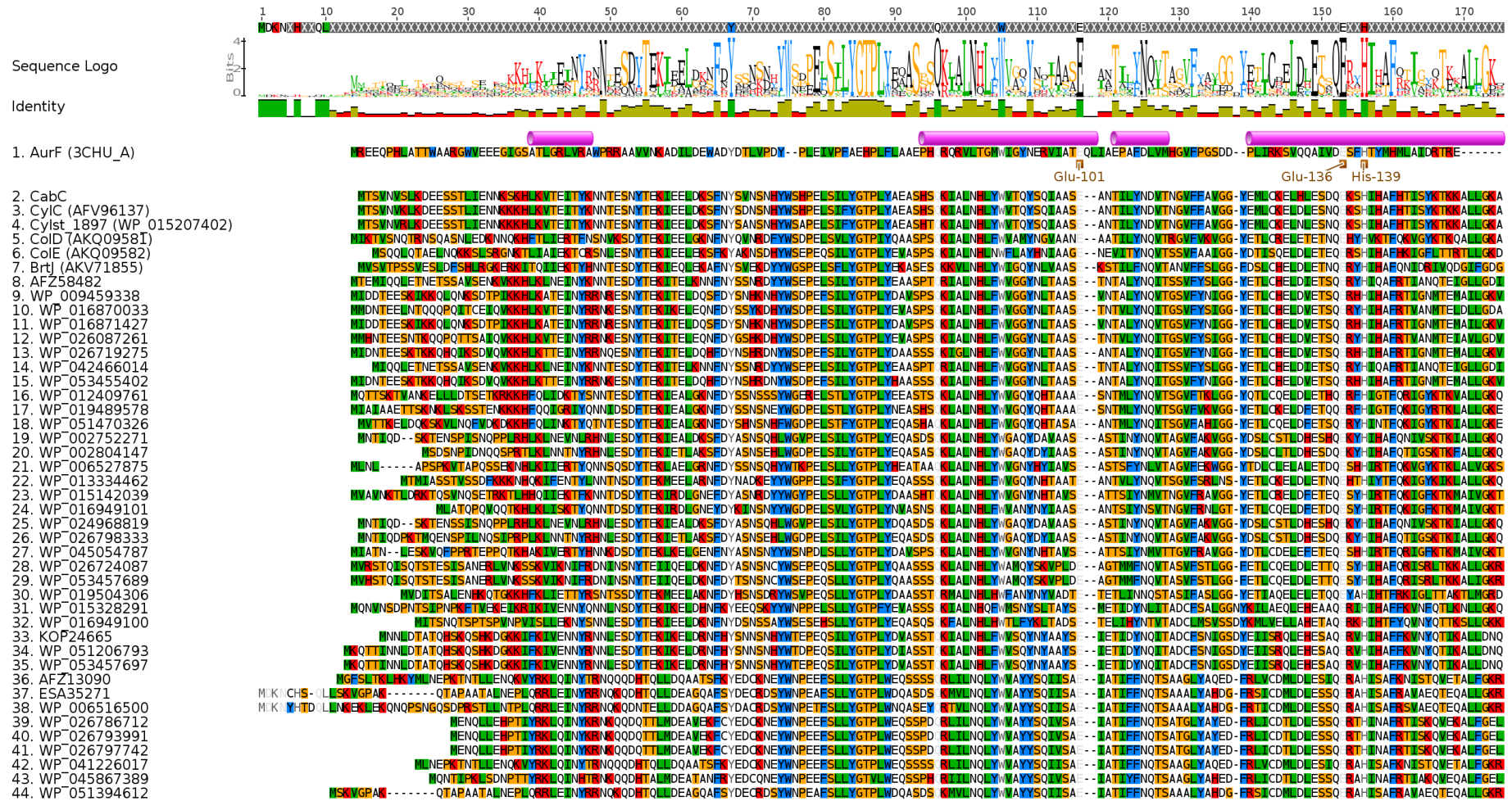


Figure S3. Cont.



Figure S3. Cont.

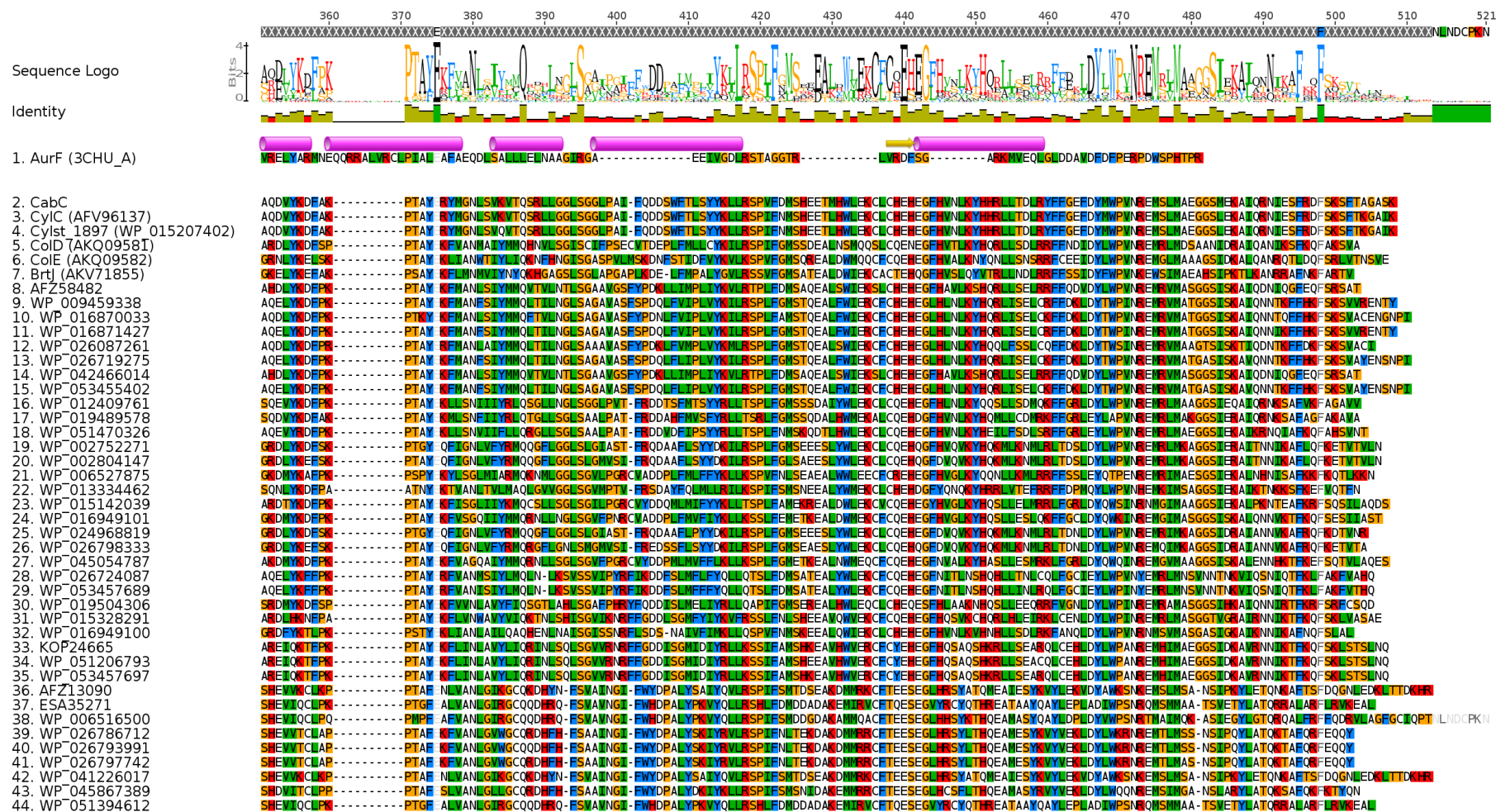


Figure S3. Protein sequence alignment of CabC and homologues. The consensus sequence based on a 100% conservation rule along with a sequence logo and an identity graph is depicted at the top. The first sequence shows the *p*-aminobenzoate *N*-oxygenase (AurF) Chain A of *Streptomyces thioluteus*. Conserved glutamic acid and histidine residues responsible for di-iron coordination are depicted below this sequence.

Table S9. Oligonucleotide primers used for gap-closure and frameshift refutation.

Name	Sequence 5'–3'	Usage ^a	Comment
MP01_129-for	GGAAATTTGAACCACCGAC	A	
MP02_129-for_seq	CCTTGAACTTTACTACTAG	S	Gap-closure between contig00129 and contig00638
MP03_638-rev_seq	AGGTATTGGATTACGAATC	S	
MP04_638-rev	AGTAGCAATAGCCGCCATC	A	
MP05_638-for	ATCTGCTTATGATGTAGCG	A	
MP06_638-for_seq	AGCATAGTGAAGTGCAGCC	S	Gap-closure between contig00638 and contig00697
MP07_697-rev_seq	TCCCTTTGTCTAGCAGGAC	S	
MP08_697-rev	GCTAAACCAACAGCATATG	A	
MP09_129-for_seq2	GAGATTCAGCAGGTTCCGG	S	Gap-closure between contig00129 and contig00638
SH1_CAVN2-F	CACCCCCTTTAGAAGACCTGG	A	
SH2_CAVN2-R	GTGCATCTTCCCAAGCCTCT	A	
SH3_CAVN2-F	GTTACAAGCCCCTAAGTTCG	S	
SH4_CAVN2-F	CGTCTAGCTGGTGTAGTGC	S	Refutation of two putative frameshifts in 454-based assembly
SH5_CAVN2-F	TCCCAAGAGAATGCAGCCAG	A, S	
SH6_CAVN2-R	GCCATCAAGCTCATTTCCTG	A, S	
SH7_CAVN2-F	GTAAGGCGCTGCAAGAAGTGC	A, S	
SH8_CAVN2-R	ATCTGGTTTGATGCCCCAGG	A, S	

^a Abbreviations: A = amplification, S = sequencing.

Table S10. Basic data of biological activity for compounds 1–30 against Gram-positive as well as Gram-negative bacteria and HaCaT cells.^a

#	MIC ($\mu\text{g/mL}$)															IC ₅₀ ($\mu\text{g/mL}$) HaCaT ^b
	<i>E. faecium</i> DSM-20477	<i>E. faecium</i> DSM-17050 (VREF)	<i>M. tuberculosis</i> ATCC 25618 (H37Rv)	<i>S. aureus</i> Newman (MSSA)	<i>S. aureus</i> N315 (MRSA)	<i>S. aureus</i> 1 (MRSA) ^b	<i>S. aureus</i> Mu50 (MRSA/VISA)	<i>S. pneumoniae</i> 7 (ATCC 49619) ^b	<i>S. pneumoniae</i> DSM-20566	<i>S. pneumoniae</i> DSM-11865 (PRSP)	<i>E. coli</i> 13 ^b	<i>E. coli</i> TolC-deficient	<i>E. coli</i> TolC-deficient +PMBN	<i>K. pneumoniae</i> 18 (KRKP) ^b	<i>P. aeruginosa</i> 22 (MDR) ^b	
1	8	2-8	8-12	1	0.25-0.5	0.08	0.5	0.2	1	2	>50	>64	2	>50	>50	2.9
2	8	4-8	2-5	0.25	0.25-0.5	nt	0.25-0.5	nt	1	0.25-0.5	nt	>64	1-2	nt	nt	nt
3	8	8	1-1.5	0.125-0.25	0.125	0.63	0.125-0.25	0.2	0.5	0.25-0.5	>50	>64	2	>50	>50	2.1
4	8	4-8	0.5-1.5	0.5	0.25-0.5	0.08	0.25	0.2	1	0.5	>50	>64	1	>50	>50	3.5
5	32	16-32	2-4	0.25	0.25	0.16	0.125	0.2	1	0.5-2	>50	>64	8-16	>50	>50	7.4
6	nt	8-16	4-8	nt	0.5	nt	nt	nt	nt	1	nt	nt	nt	nt	nt	nt
7	2	2	0.5-1.5	0.125	0.06-0.125	0.04	0.125	0.2	0.25	0.25	>50	>64	1	>50	>50	2.4
8	4	4	2-5	0.25	0.125-0.25	nt	0.25	nt	0.5-1	0.5	nt	>64	1	nt	nt	nt
9	8	4	0.5-2	0.125-0.25	0.125	0.16	0.5	0.2	0.25-0.5	0.25	>50	>64	1	>50	>50	7.5
10	4	4	2-3	0.125-0.25	0.125	0.08	0.125-0.25	0.2	0.5-1	0.25-0.5	>50	>64	1-2	>50	>50	4.0
11	nt	8	2-4	nt	0.25	0.08	nt	0.2	nt	0.25	>50	nt	nt	>50	>50	2.2
12	4	2-4	2-4	0.125-0.25	0.125	0.08	0.125	0.2	0.25-0.5	0.25	>50	>64	1	>50	>50	2.1
13	4	4	1-1.5	0.125-0.25	0.125	0.08	0.125	0.2	0.25-0.5	0.125-0.25	>50	>64	1	>50	>50	3.4
14	4	4	32-64	0.25	0.125	0.08	0.125-0.5	0.2	0.25-0.5	0.25-0.5	>50	>64	1-2	>50	>50	3.9
15	nt	4	2-3	nt	0.25	0.08	nt	0.2	nt	0.5	>50	nt	nt	>50	>50	3.8
16	2	2	1.5-2	0.125-0.25	0.06-0.125	0.08	0.125	0.2	0.25	0.5	>50	>64	0.5-1	>50	>50	2.7
17	2	2	2-5	0.125-0.25	0.06-0.125	0.08	0.125	0.2	0.25	0.25	>50	>64	0.5	>50	>50	3.4
18	2-4	2	1-1.5	0.125	0.06	0.08	0.125	0.2	0.25	0.25	>50	>64	0.5-1	>50	>50	3.6
19	4-8	8	2-3	0.125	0.125	0.08	0.125	0.2	0.5	0.25	>50	>64	1-4	>50	>50	2.5
20	nt	2	1.5-2	nt	0.125-0.25	0.08	nt	0.2	nt	0.25	>50	nt	nt	>50	>50	4.8
21	nt	8	>8	1-2	0.5	0.63	8	1.3	nt	2	>50	>64	4-8	>50	>50	7.0
22	nt	nt	>8	nt	nt	0.63	nt	1.3	nt	nt	>50	nt	nt	>50	>50	7.5
23	nt	4-8	2-4	0.5	0.5	0.31	1	0.63	nt	nt	>50	>64	2	>50	>50	5.9
24	nt	nt	>8	nt	nt	0.31	nt	0.63	nt	nt	>50	nt	nt	>50	>50	6.7
25	4	2	2-4	0.125	0.125	0.26	0.125	0.57	0.25	0.25	>50	>64	1-2	>50	>50	2.9
26	4	2	0.5-1	0.125	0.125	0.08	0.125	0.2	0.5	0.125	>50	>64	2-4	>50	>50	1.8
27	8	2	1-2	1-4	0.5-2	0.63	2-8	1.6	2-8	4-8	>50	>64	64	>50	>50	7.3
28	16	16	>16	4	4-8	3.2	4-8	6.23	4	4	>50	>64	4	>50	>50	37.3
29	64	64	>16	2-4	4	>50	4-8	>50	2-8	2	>50	>64	8-32	>50	>50	16.5
30	>64	>64	>16	4-8	>64	>50	>64	>50	4	2-4	>50	>64	>64	>50	>50	17.5
POS	2.0 ^c	>64 ^c	0.024-0.036 ^d 0.125-0.25 ^e 0.02-0.08 ^f 0.2-0.8 ^g	0.5 ^c	1.0 ^c	2.0 ^{ch}	16 ^c	2.0 ^{ch}	<0.03 ⁱ	>64 ⁱ	0.0062 ^j 62.5 ^c	0.003 ^j	0.003 ^j	1.25 ^j 0.62 ^k	0.025 ^l 250 ^c	3.9 ^m

^a Abbreviations: VREF = vancomycin-resistant *E. faecium*, MSSA = methicillin-sensitive *S. aureus*, MRSA = methicillin-resistant *S. aureus*, VISA = vancomycin-intermediate *S. aureus*, PRSP = penicillin-resistant *S. pneumoniae*, PMBN = polymyxin B nonapeptide, KRKP = kanamycin-resistant *K. pneumoniae*, MDR = multi-drug resistant (for detailed resistance profile, see Pretsch *et al.* [4]), n.t. = not tested, POS = positive control; ^b Equivalent data for 10–30 have previously been reported; For further details, see Preisitsch *et al.* [5] (10–25) and Preisitsch *et al.* [6] (26–30); ^c vancomycin; ^d delamanid; ^e pretomanid (formerly known as PA-824); ^f isoniazid; ^g rifampicin; ^h fusidic acid; ⁱ ampicillin; ^j ciprofloxacin; ^k moxifloxacin; ^l levofloxacin; ^m mitoxantrone.

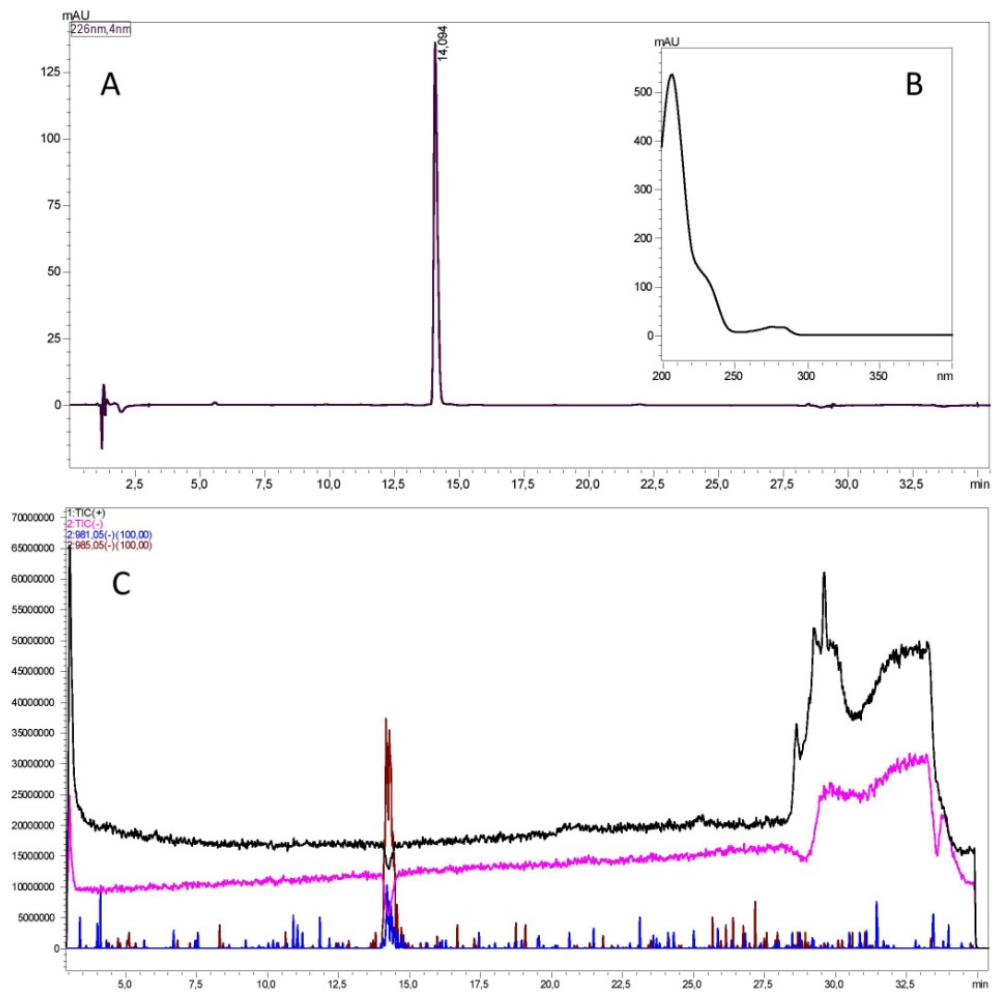


Figure S4. Cont.

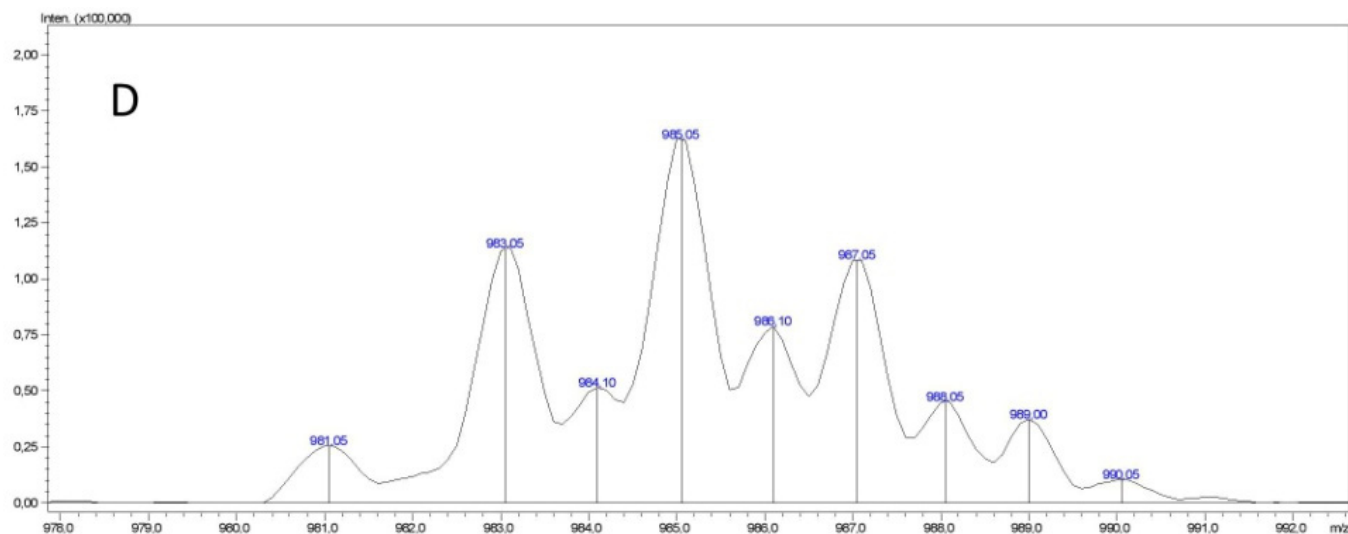


Figure S4. Identity and stability control of carbamidocyclophane Q (**5**) after the antimycobacterial bioactivity assay. HPLC-UV-MS analysis was performed on a Shimadzu LC-20A Prominence liquid chromatography system with a SPD-M20A diode array detector (DAD) coupled to a Shimadzu LCMS-8030 triple quadrupole (QqQ) mass spectrometer using a Phenomenex Kinetex PFP column (100 × 4.6 mm, 2.6 μm, 100 Å) and a binary gradient of MeOH in deionized H₂O with a flow rate of 0.8 mL/min from 60% to 80.3% MeOH in 26 min at 40 °C. Sample: 0.1 mg of **5** in 1.0 mL MeOH, 10 μL injection, solvent flow split of 10:1 after the DAD analysis and prior to QqQ measurement. (A) HPLC chromatogram of **5** detected at wavelength λ = 226 nm; (B) Online UV spectrum (λ from 200 to 400 nm) of **5** at retention time 14.1 min; (C) Total ion chromatograms (TICs) of **5** (positive mode in black and negative mode in magenta) and its extracted ion chromatograms (EICs) for *m/z* 981.05 and 985.05 (both negative mode), consistent with the monoisotopic mass peak [M – H][–] and the most abundant isotopic mass peak [M + 4 – H][–], respectively; (D) Measured isotopic distribution pattern of **5** referring to the [M – H][–] ion.

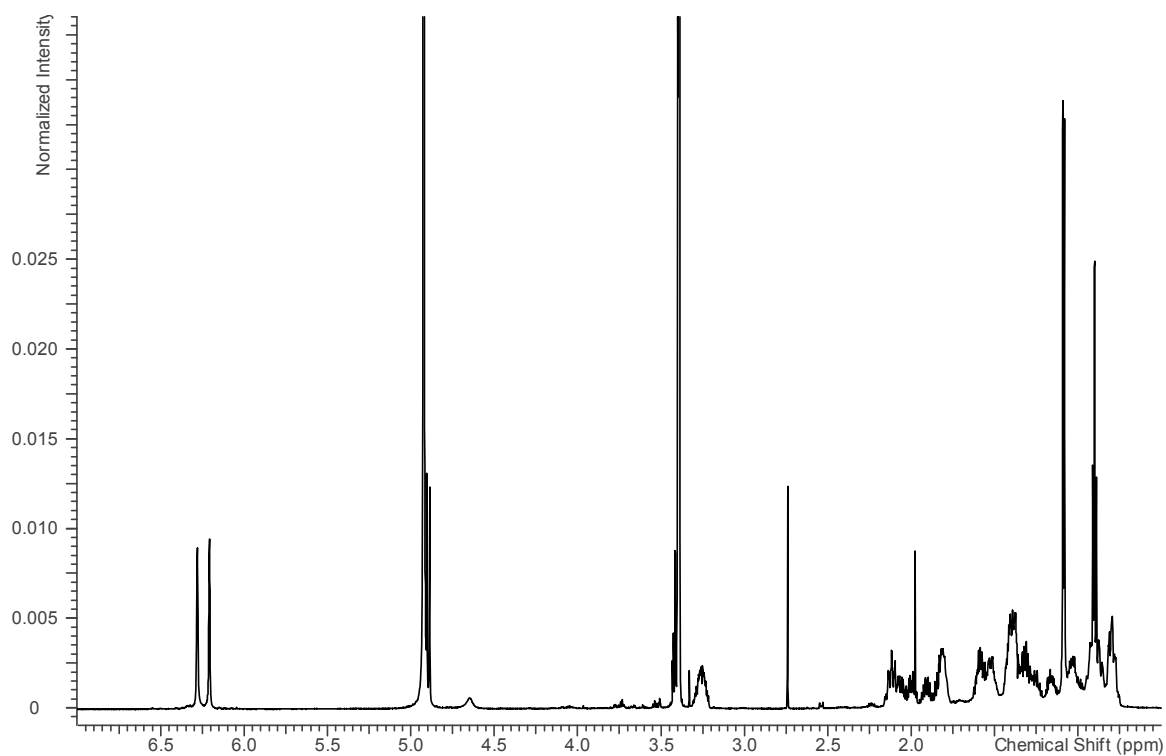


Figure S5. ^1H NMR spectrum (600 MHz, $\text{MeOH-}d_4$) of carbamidocyclophane M (1).

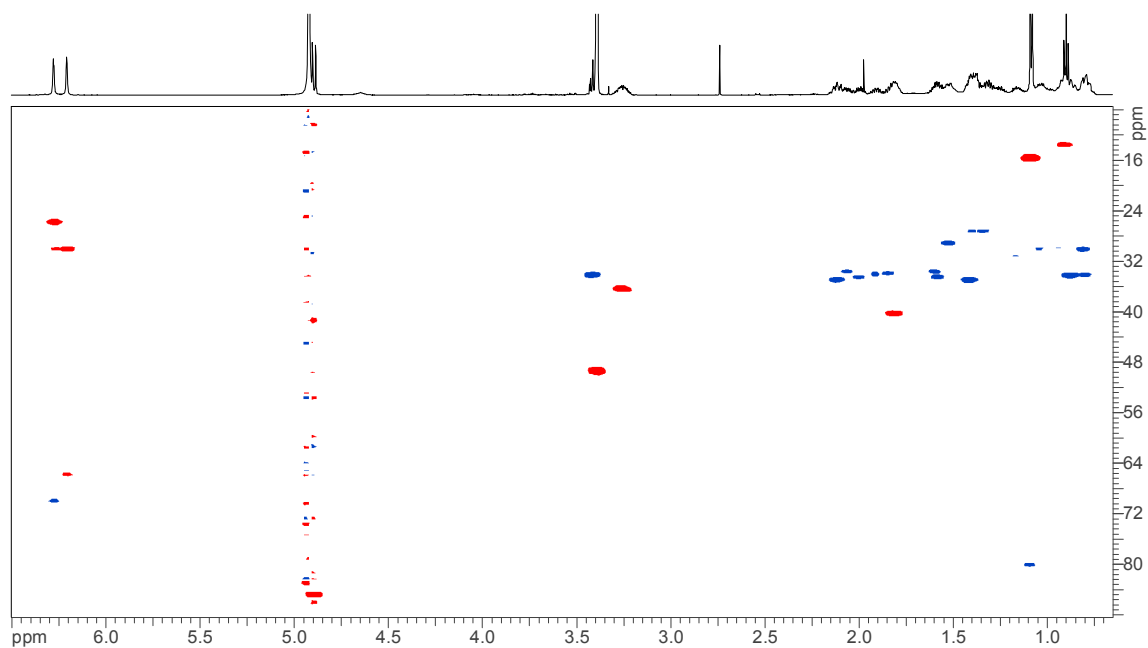


Figure S6. HMQC-DEPT spectrum (600 MHz, $\text{MeOH-}d_4$) of carbamidocyclophane M (1). Red signals are attributed to CH or CH_3 groups (positively phased) and blue signals to CH_2 groups (negatively phased).

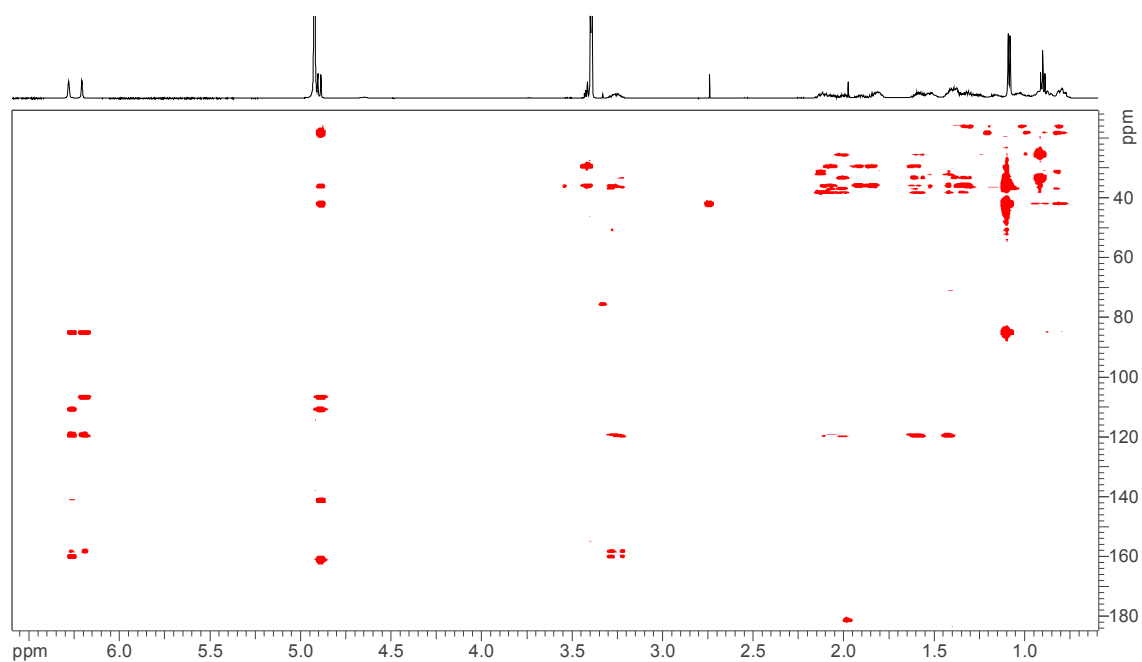


Figure S7. HMBC spectrum (600 MHz, MeOH-*d*₄) of carbamidocyclophane M (**1**).

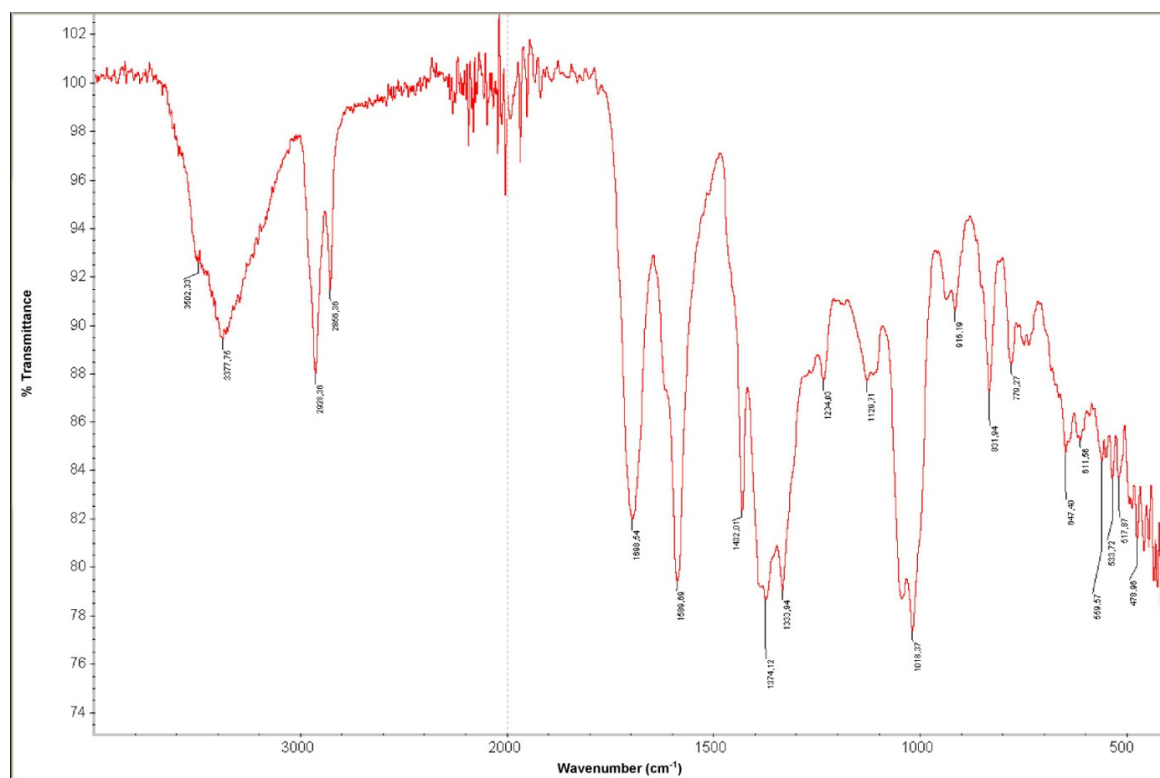


Figure S8. ATR-IR (film) spectrum of carbamidocyclophane M (**1**).

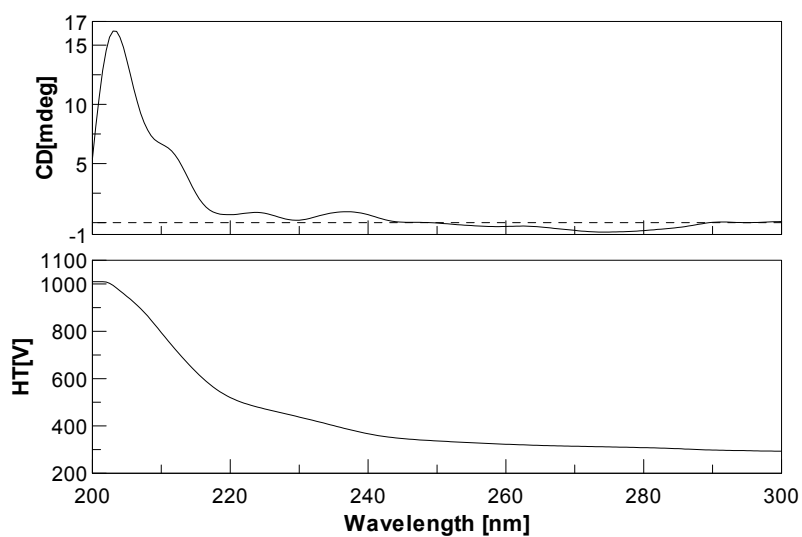


Figure S9. ECD spectrum of carbamidocyclophane M (1).

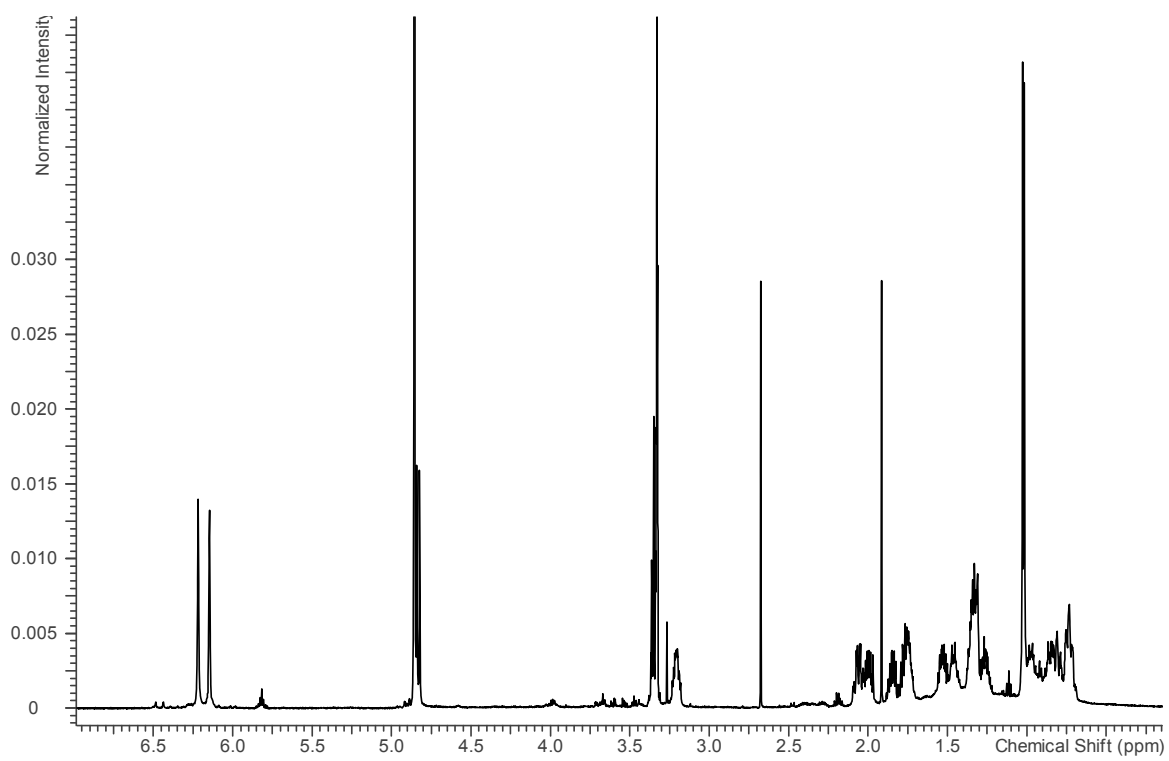


Figure S10. ^1H NMR spectrum (600 MHz, $\text{MeOH-}d_4$) of carbamidocyclophane N (2).

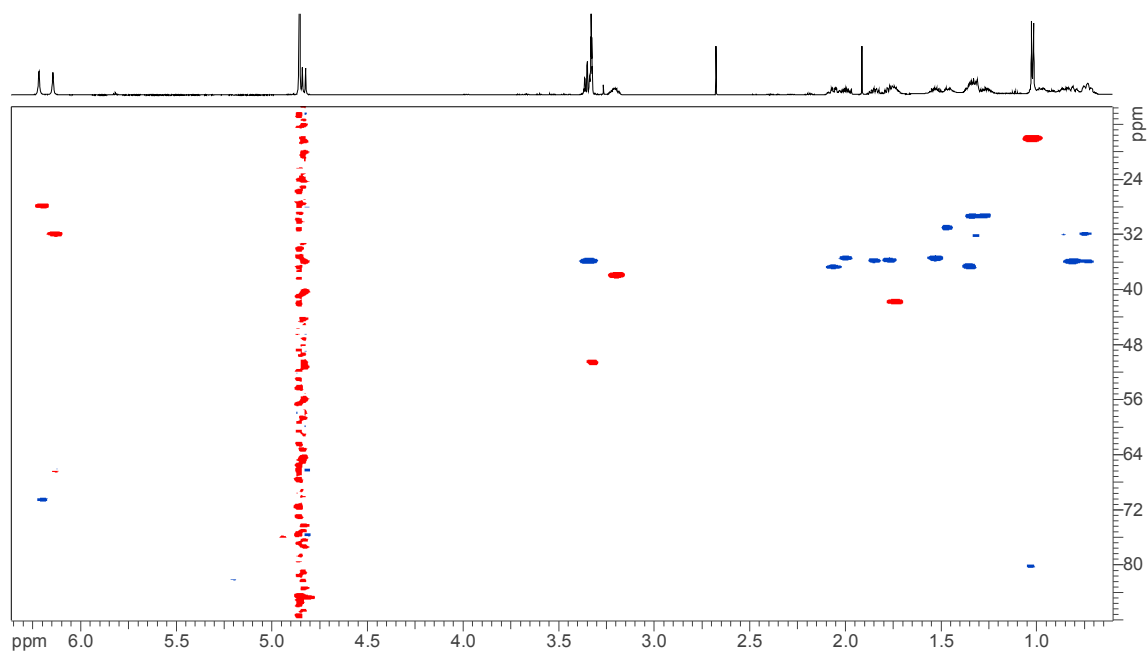


Figure S11. HMQC-DEPT spectrum (600 MHz, $\text{MeOH-}d_4$) of carbamidocyclophane N (**2**). Red signals are attributed to CH or CH_3 groups (positively phased) and blue signals to CH_2 groups (negatively phased).

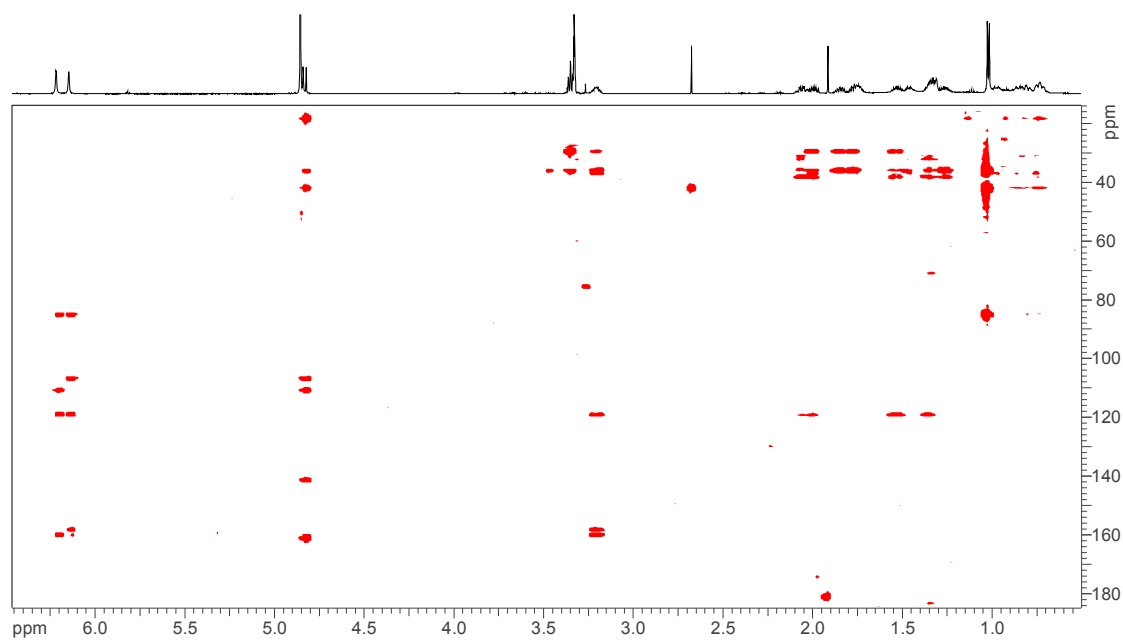


Figure S12. HMBC spectrum (600 MHz, $\text{MeOH-}d_4$) of carbamidocyclophane N (**2**).

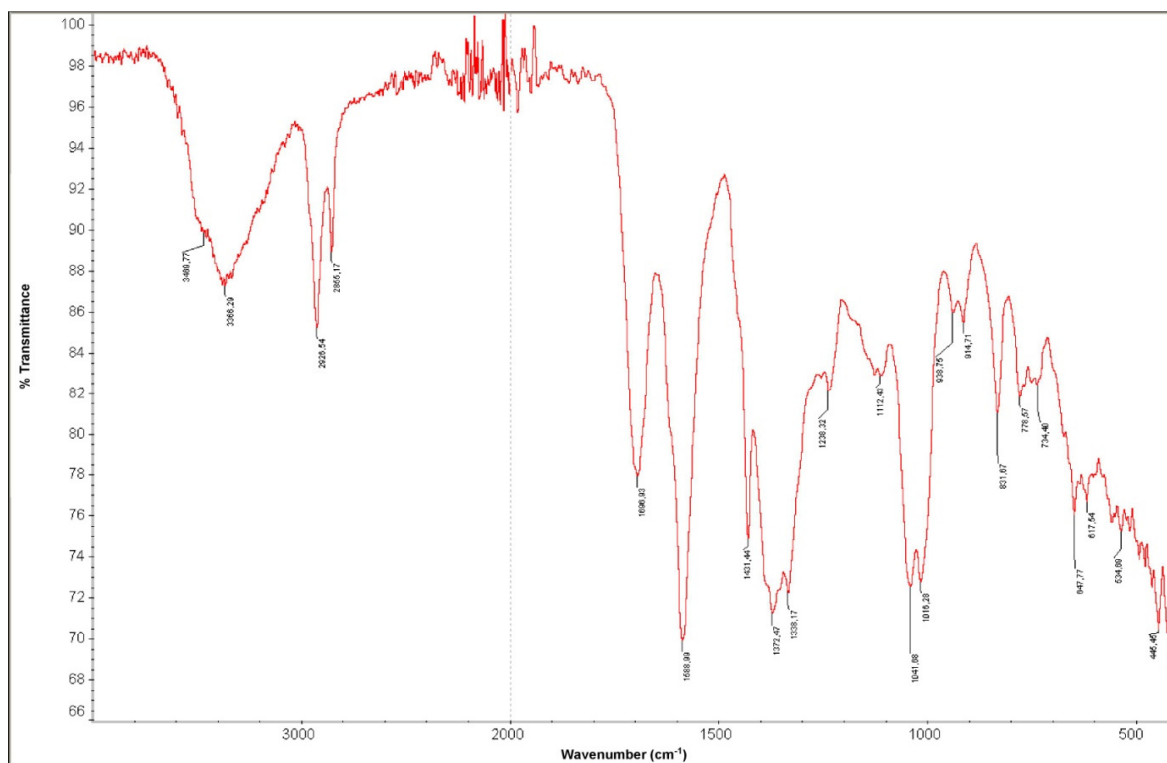


Figure S13. ATR-IR (film) spectrum of carbamidocyclophane N (2).

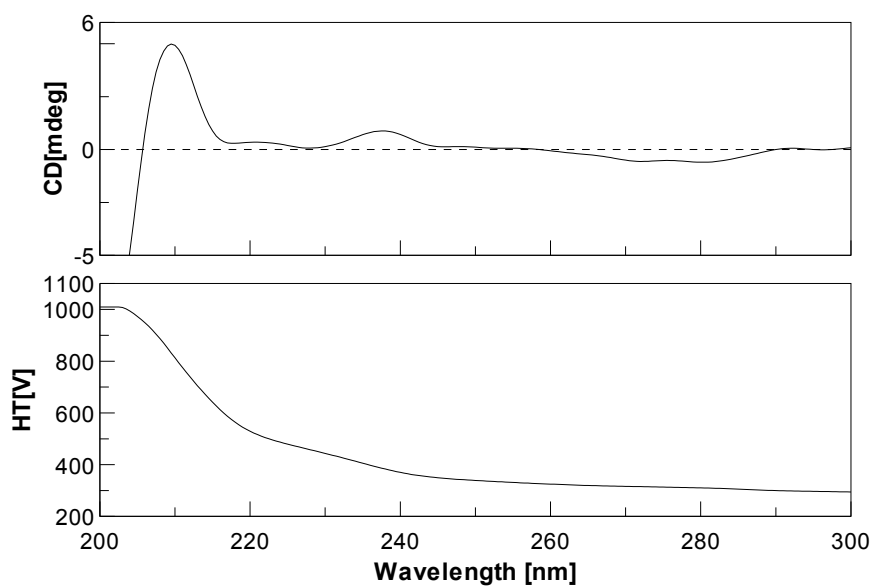


Figure S14. ECD spectrum of carbamidocyclophane N (2).

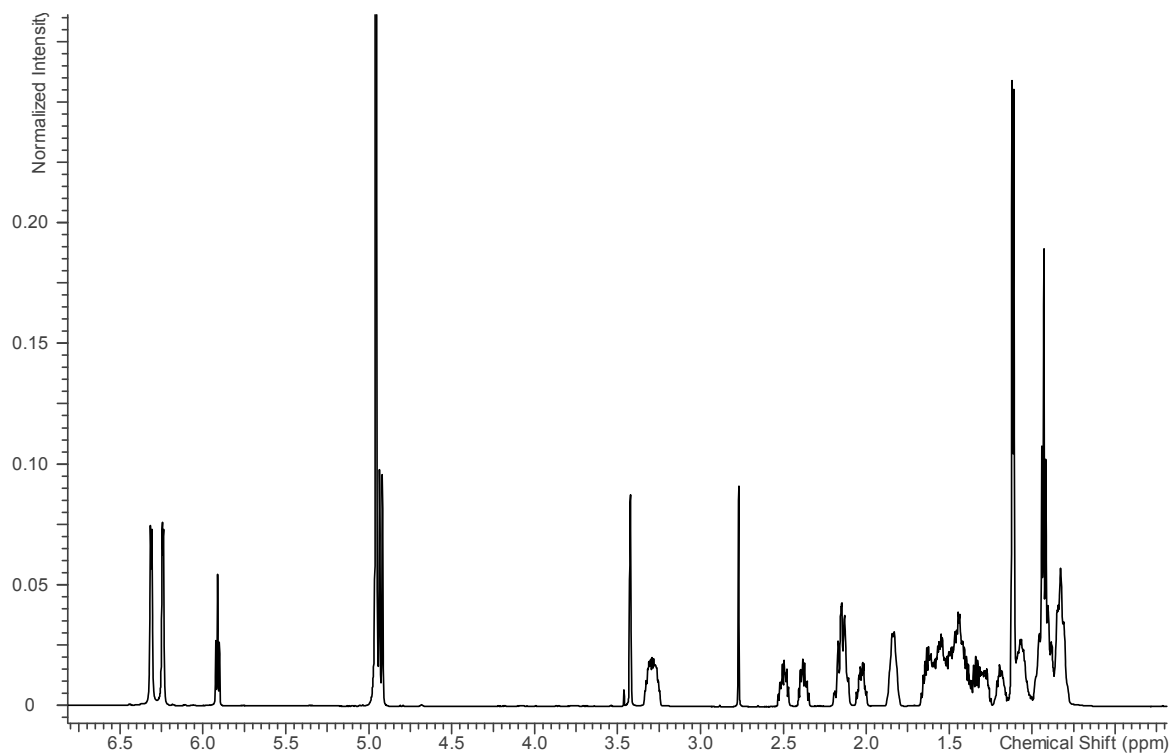


Figure S15. ^1H NMR spectrum (600 MHz, $\text{MeOH-}d_4$) of carbamidocyclophane O (3).

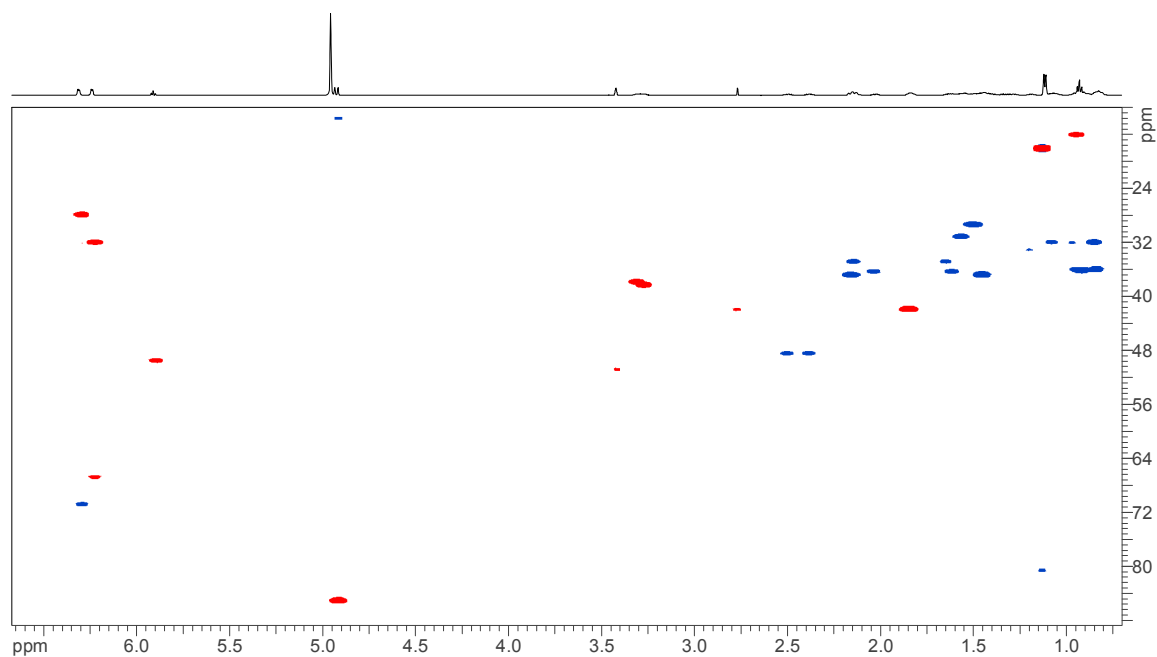


Figure S16. HMQC-DEPT spectrum (600 MHz, $\text{MeOH-}d_4$) of carbamidocyclophane O (3). Red signals are attributed to CH or CH_3 groups (positively phased) and blue signals to CH_2 groups (negatively phased).

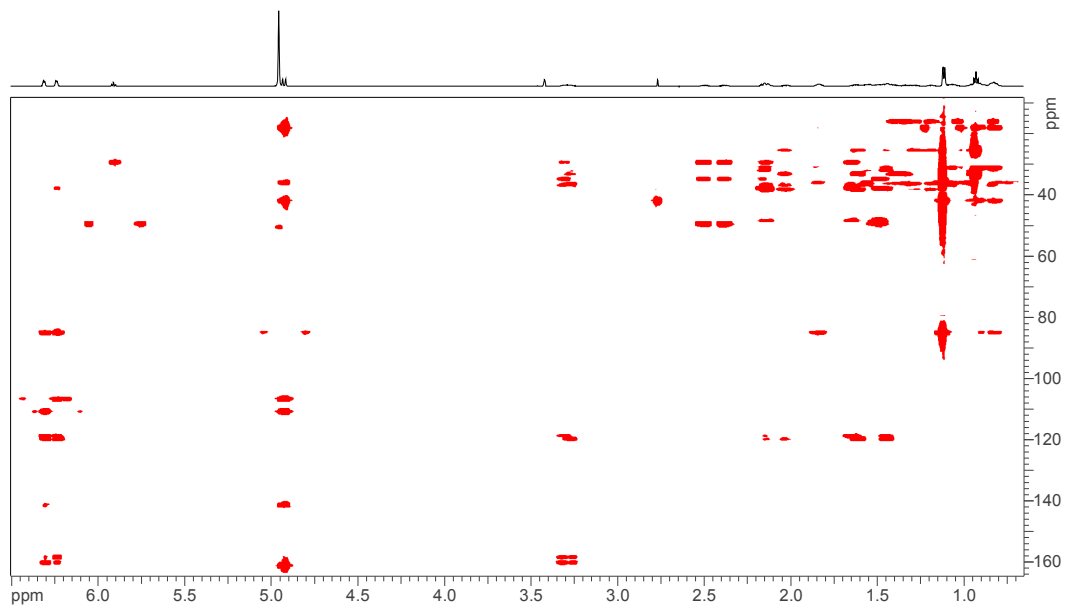


Figure S17. HMBC spectrum (600 MHz, MeOH-*d*₄) of carbamidocyclophane O (3).

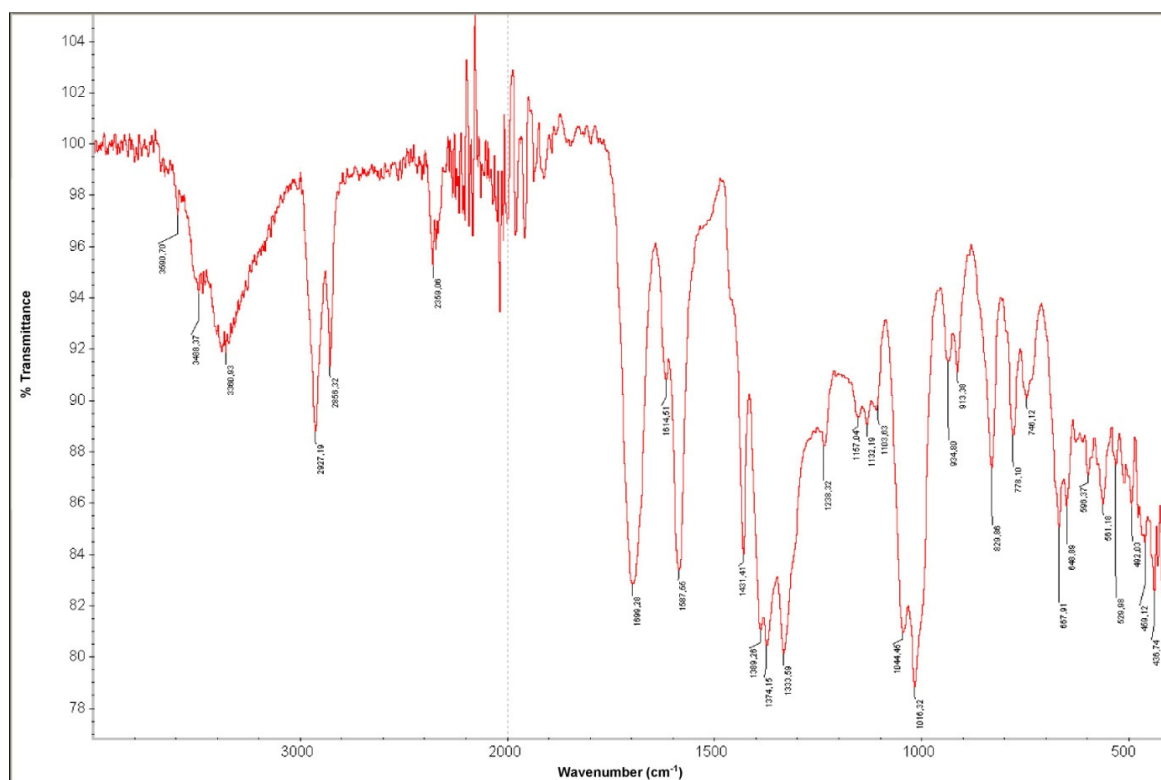


Figure S18. ATR-IR (film) spectrum of carbamidocyclophane O (3).

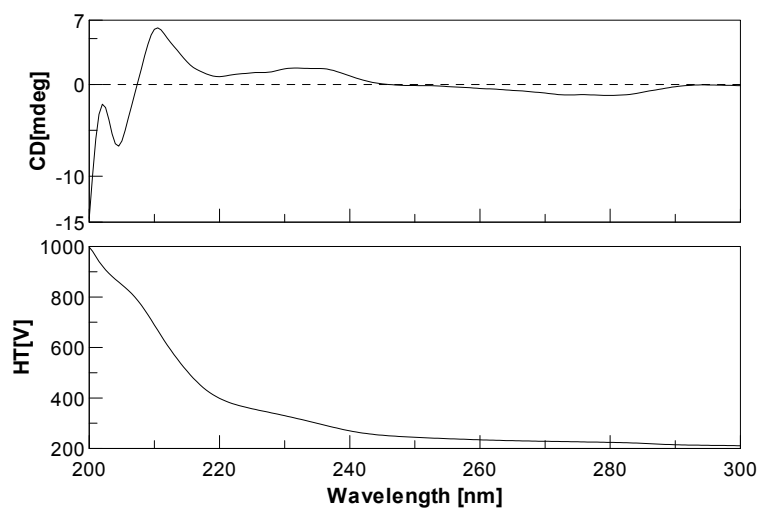


Figure S19. ECD spectrum of carbamidocyclophane O (3).

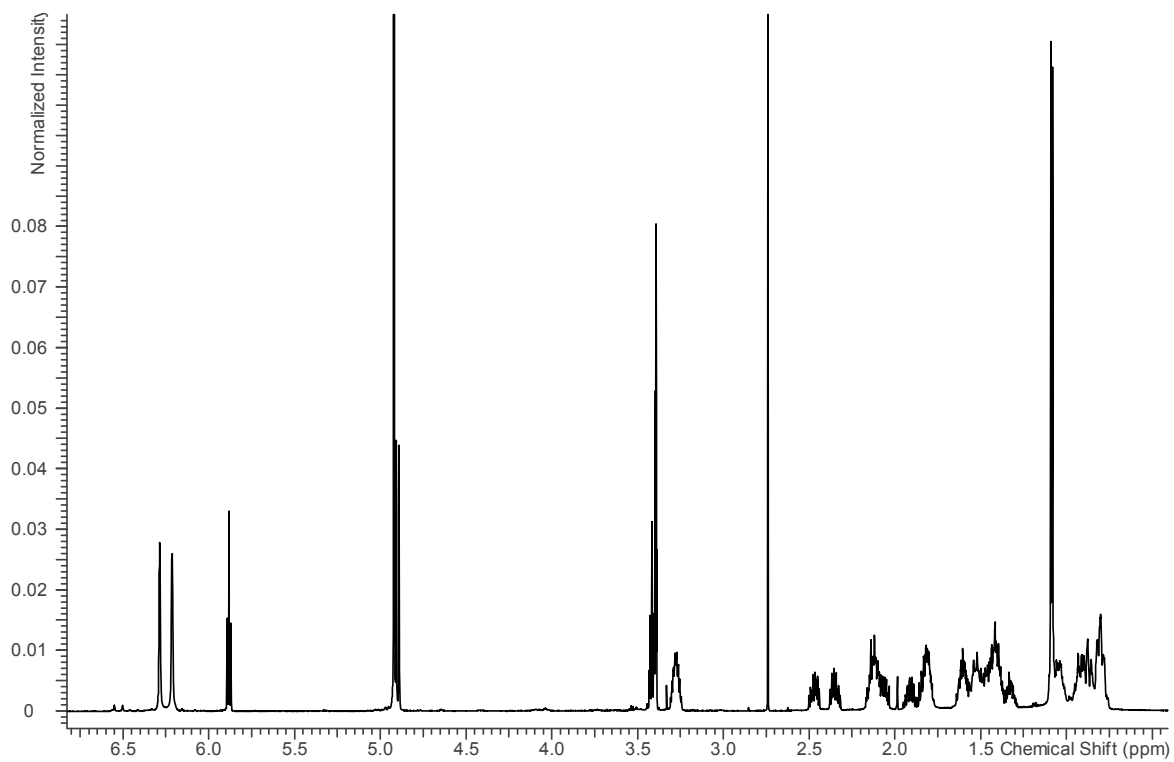


Figure S20. ¹H NMR spectrum (600 MHz, MeOH-*d*₄) of carbamidocyclophane P (4).

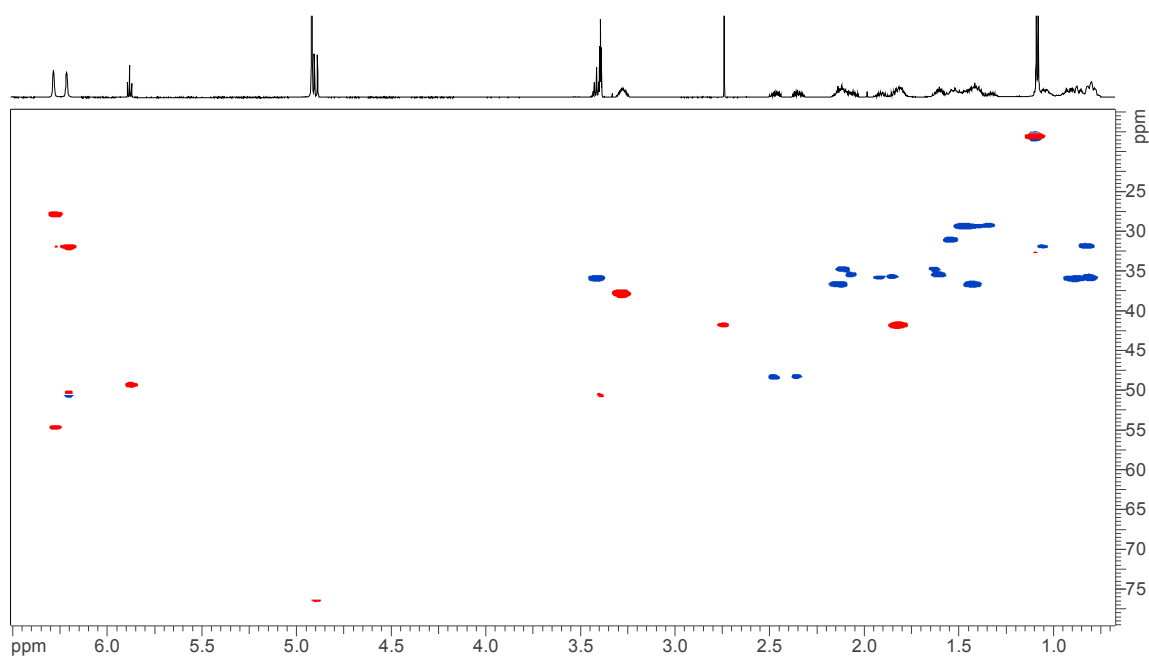


Figure S21. HMQC-DEPT spectrum (600 MHz, $\text{MeOH-}d_4$) of carbamidocyclophane P (4). Red signals are attributed to CH or CH_3 groups (positively phased) and blue signals to CH_2 groups (negatively phased).

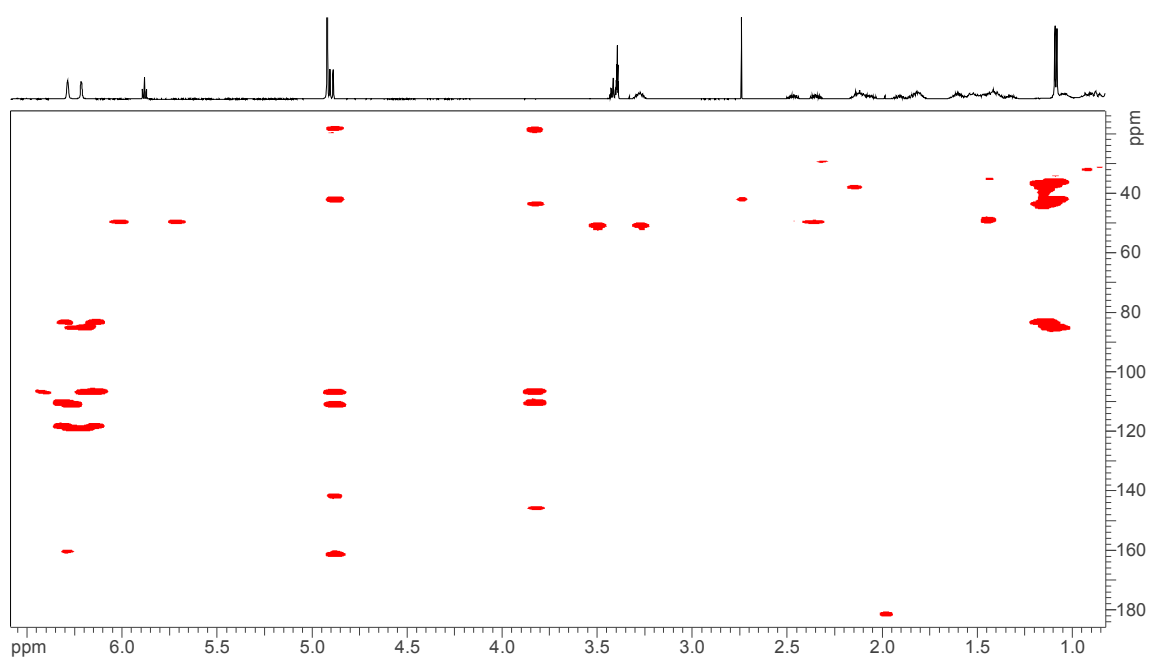


Figure S22. HMBC spectrum (600 MHz, $\text{MeOH-}d_4$) of carbamidocyclophane P (4).

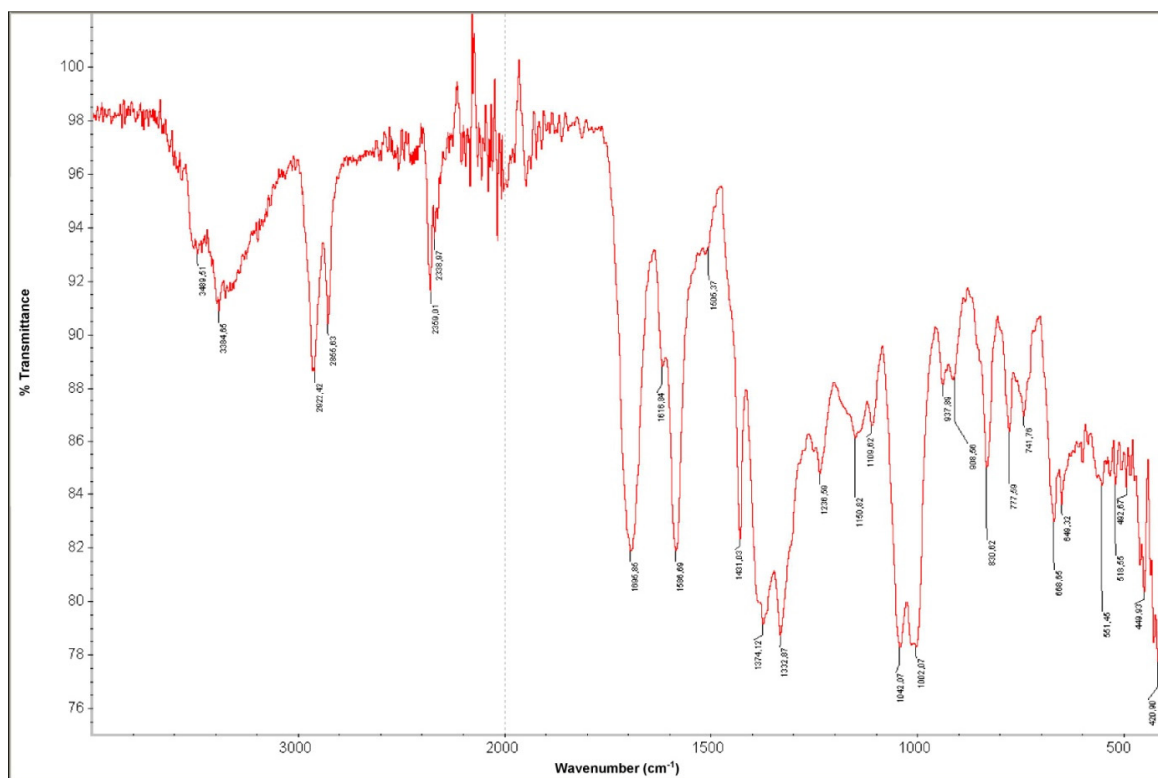


Figure S23. ATR-IR (film) spectrum of carbamidocyclophane P (4).

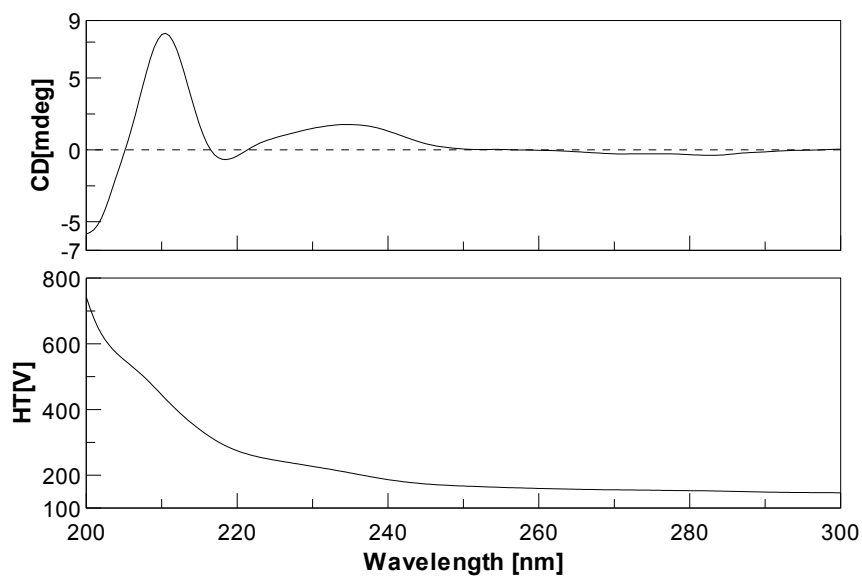


Figure S24. ECD spectrum of carbamidocyclophane P (4).

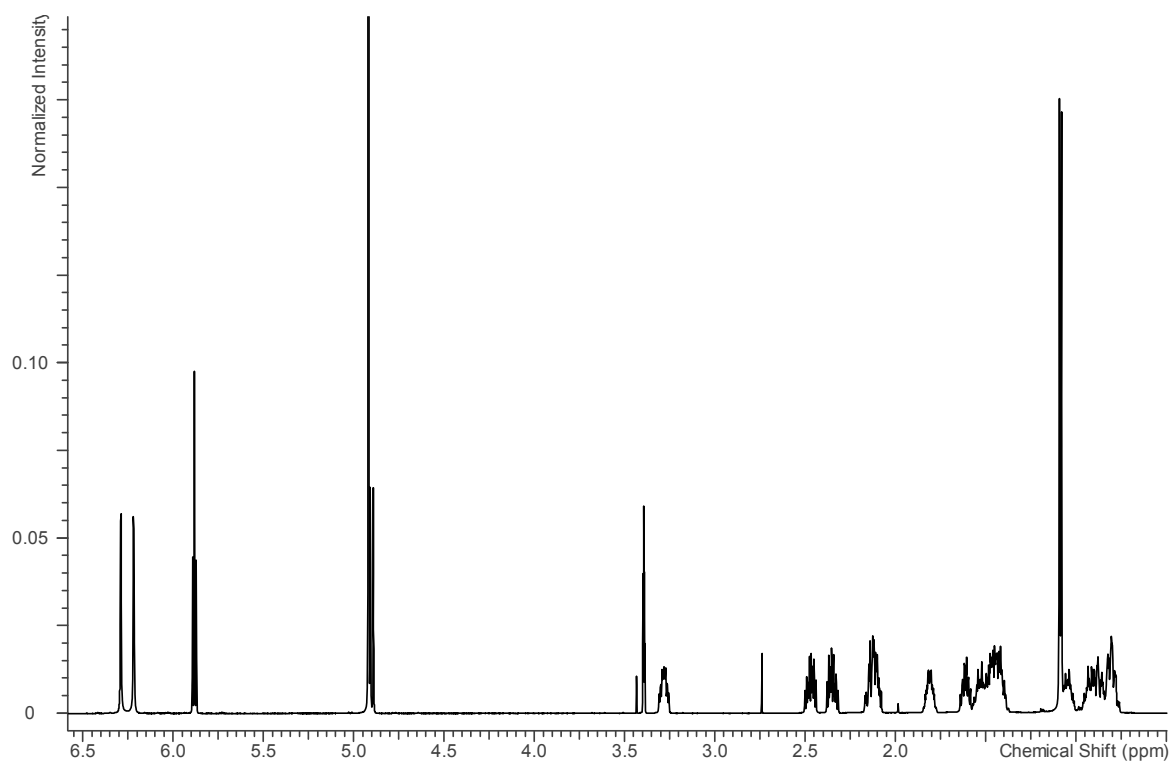


Figure S25. ^1H NMR spectrum (600 MHz, $\text{MeOH-}d_4$) of carbamidocyclophane Q (5).

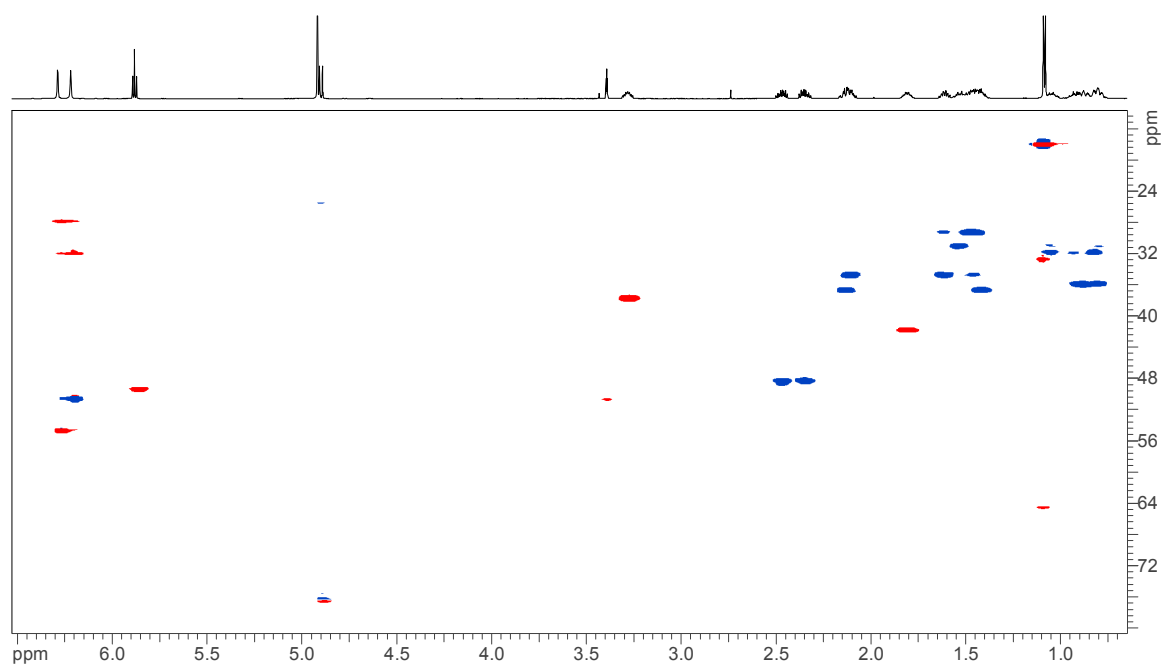


Figure S26. HMOC-DEPT spectrum (600 MHz, $\text{MeOH-}d_4$) of carbamidocyclophane Q (5). Red signals are attributed to CH or CH_3 groups (positively phased) and blue signals to CH_2 groups (negatively phased).

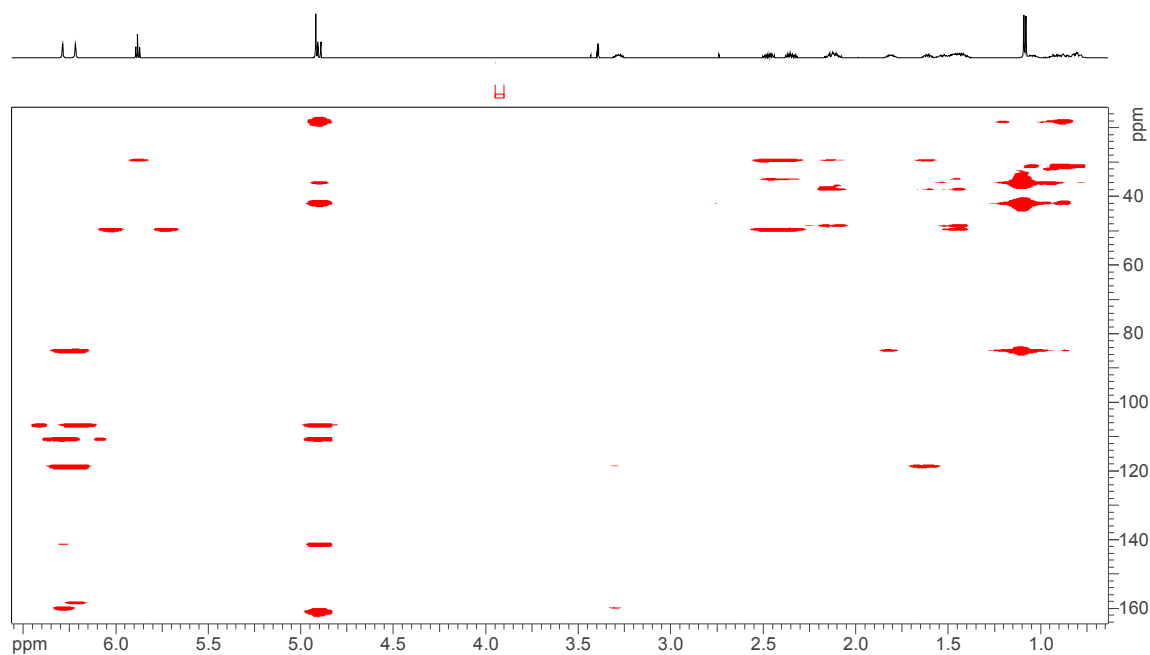


Figure S27. HMBC spectrum (600 MHz, MeOH-*d*₄) of carbamidocyclophane Q (5).

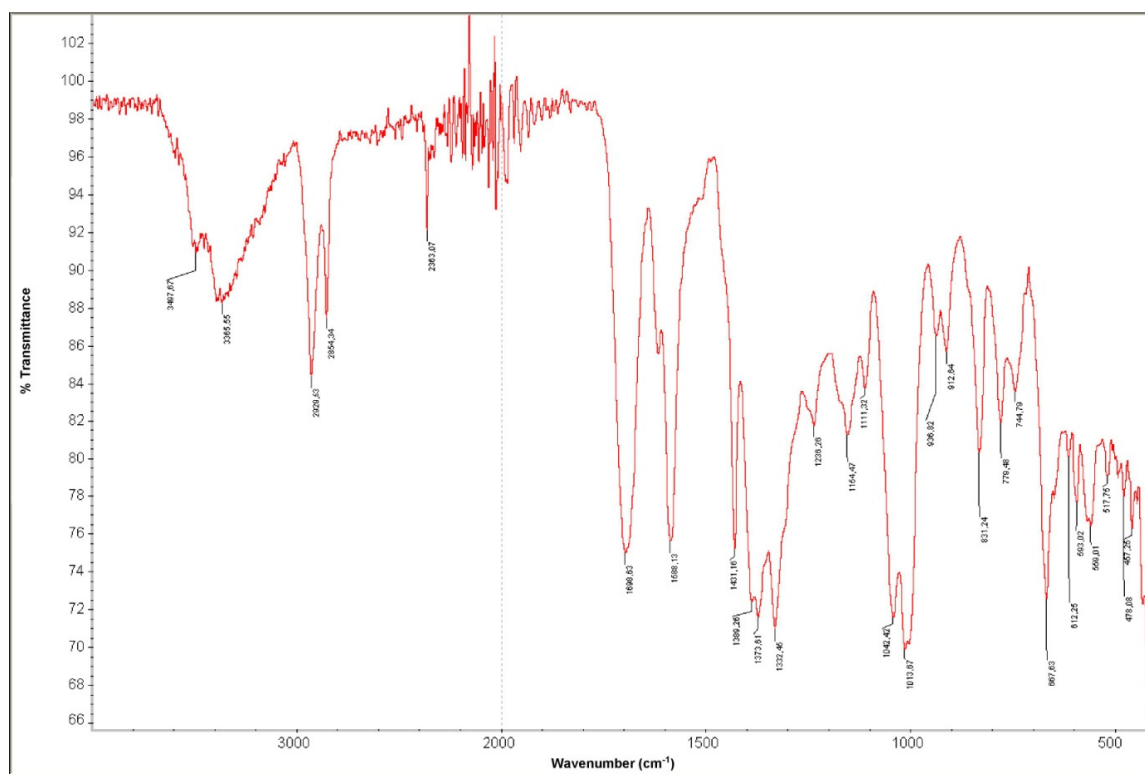


Figure S28. ATR-IR (film) spectrum of carbamidocyclophane Q (5).

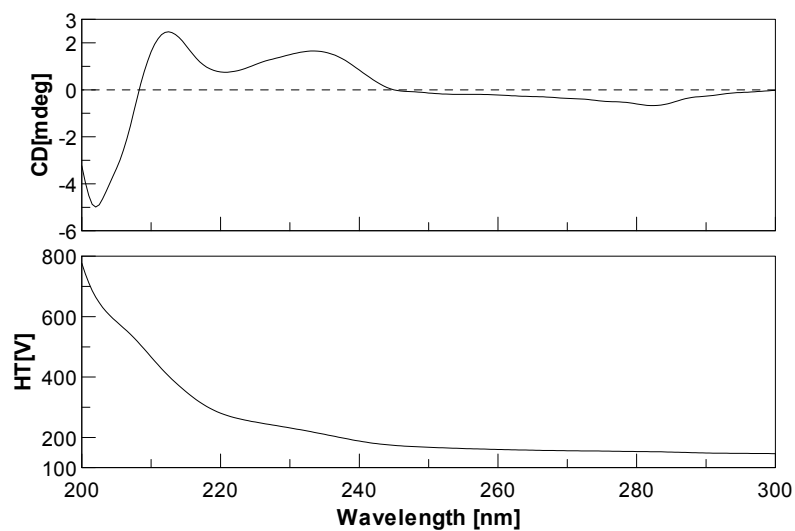


Figure S29. ECD spectrum of carbamidocyclophane Q (5).

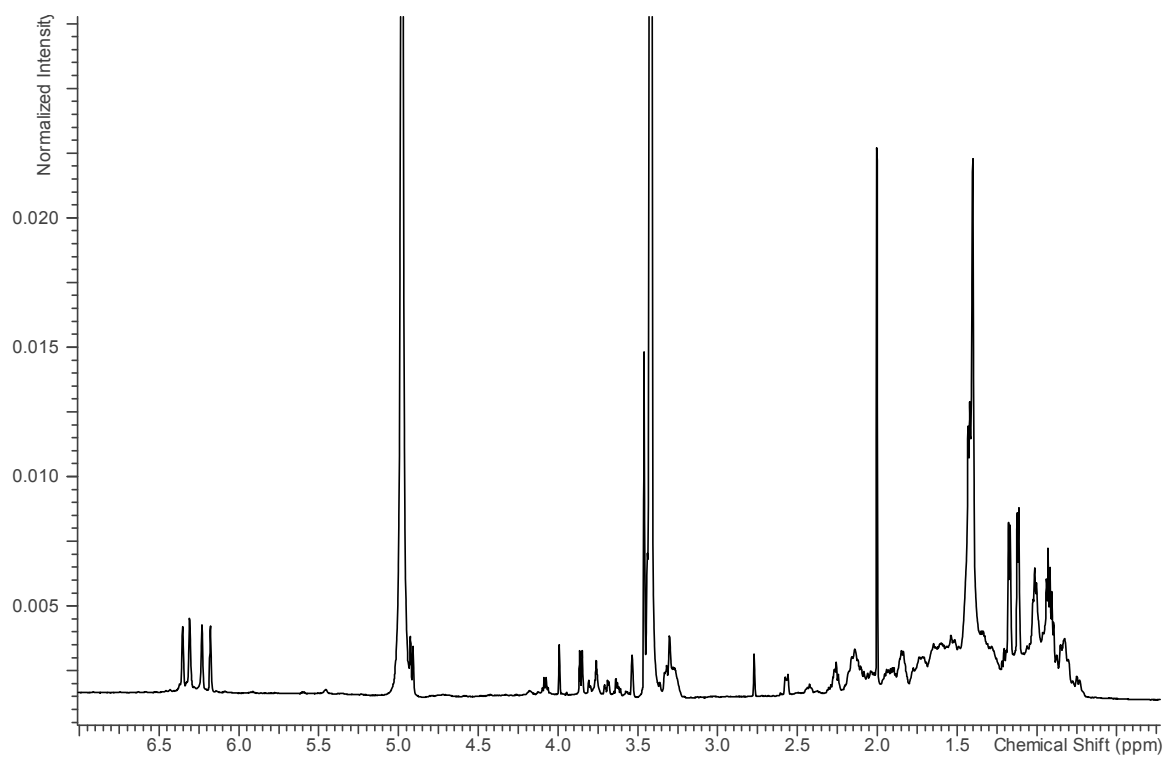


Figure S30. ¹H NMR spectrum (600 MHz, MeOH-*d*₄) of carbamidocyclophane R (6).

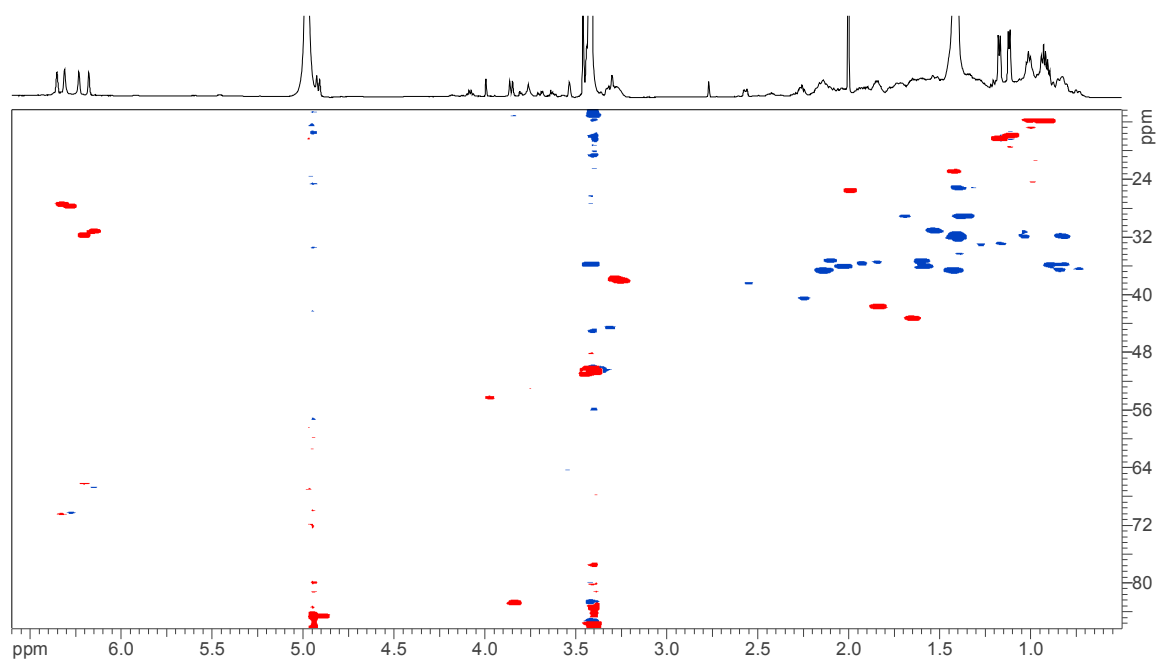


Figure S31. HMQC-DEPT spectrum (600 MHz, MeOH-*d*₄) of carbamidocyclophane R (**6**). Red signals are attributed to CH or CH₃ groups (positively phased) and blue signals to CH₂ groups (negatively phased).

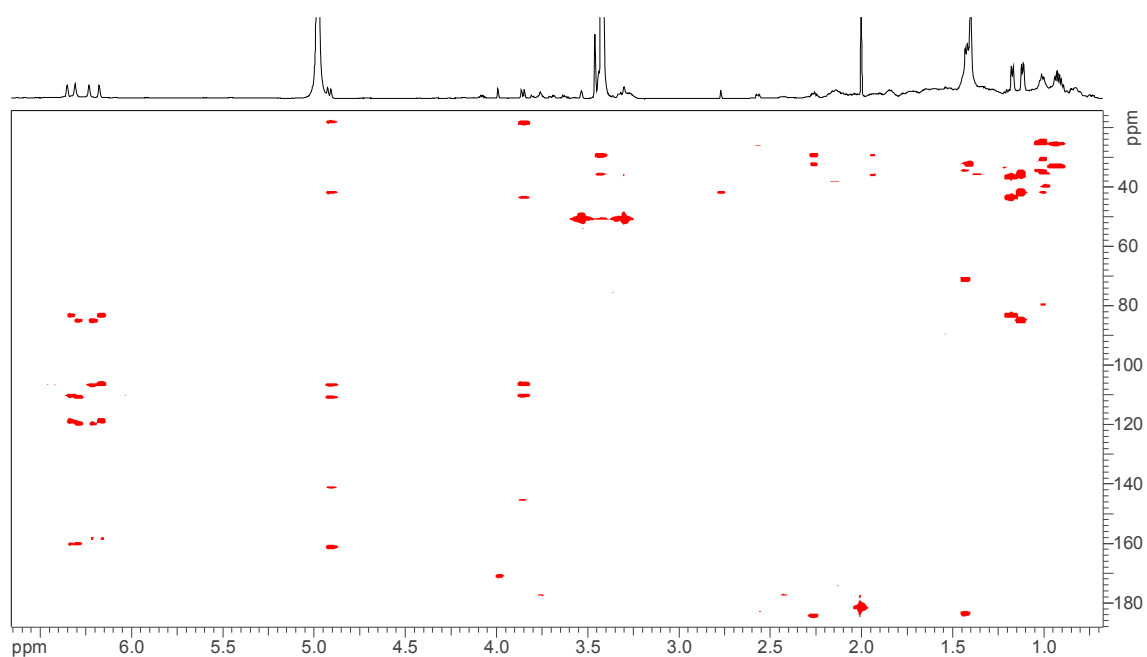


Figure S32. HMBC spectrum (600 MHz, MeOH-*d*₄) of carbamidocyclophane R (**6**).

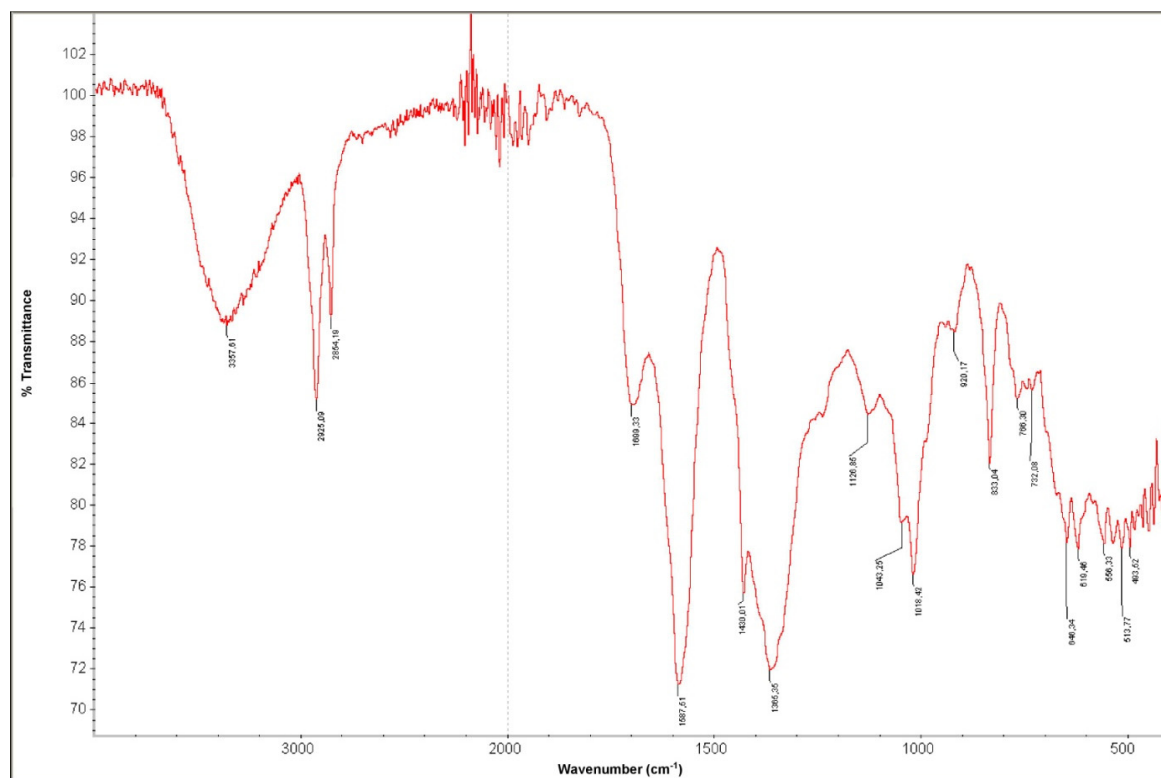


Figure S33. ATR-IR (film) spectrum of carbamidocyclophane R (6).

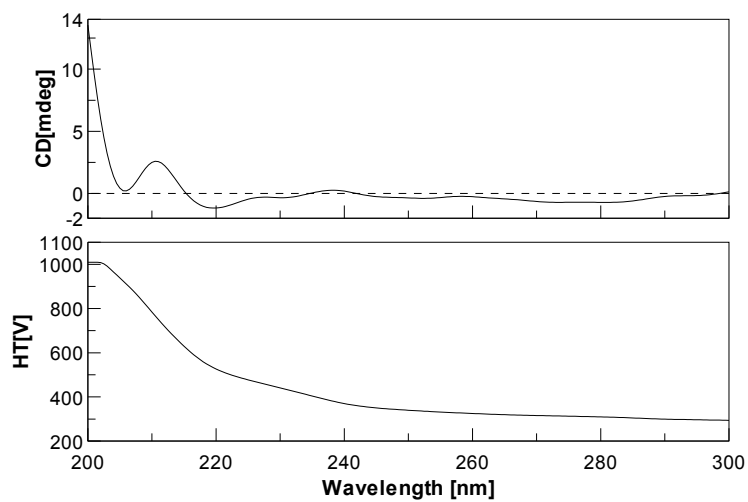


Figure S34. ECD spectrum of carbamidocyclophane R (6).

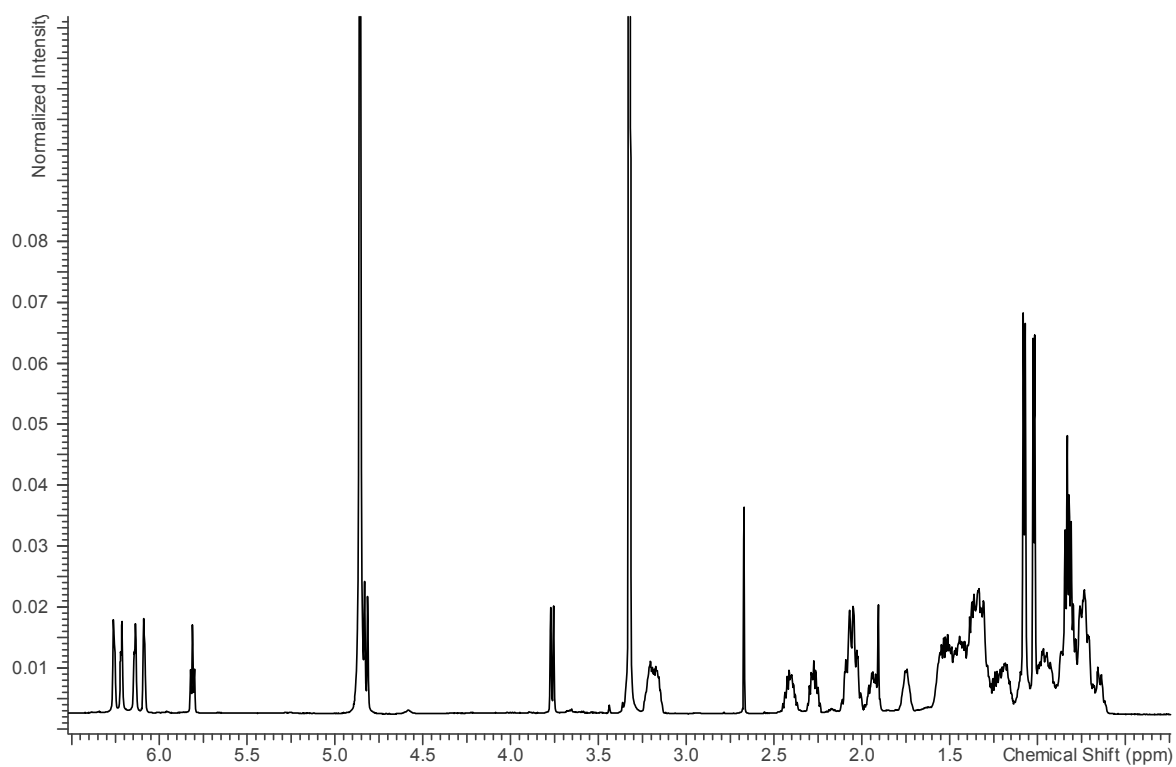


Figure S35. ^1H NMR spectrum (600 MHz, $\text{MeOH-}d_4$) of carbamidocyclophane S (7).

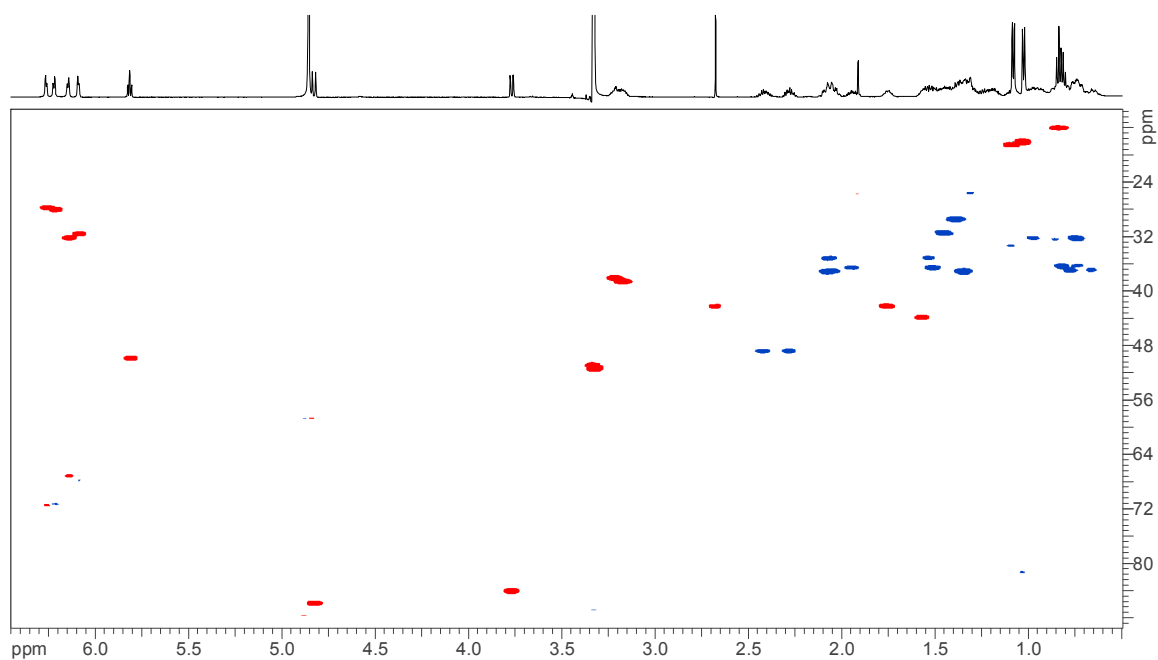


Figure S36. HMOC-DEPT spectrum (600 MHz, $\text{MeOH-}d_4$) of carbamidocyclophane S (7). Red signals are attributed to CH or CH_3 groups (positively phased) and blue signals to CH_2 groups (negatively phased).

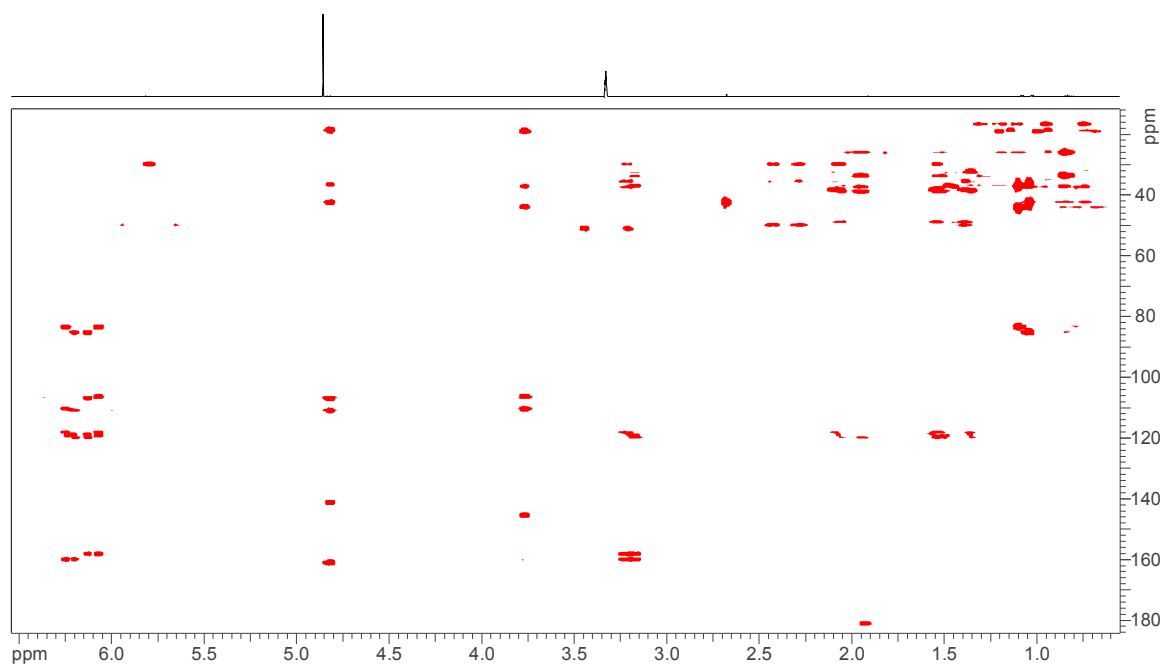


Figure S37. HMBC spectrum (600 MHz, MeOH-*d*₄) of carbamidocyclophane S (7).

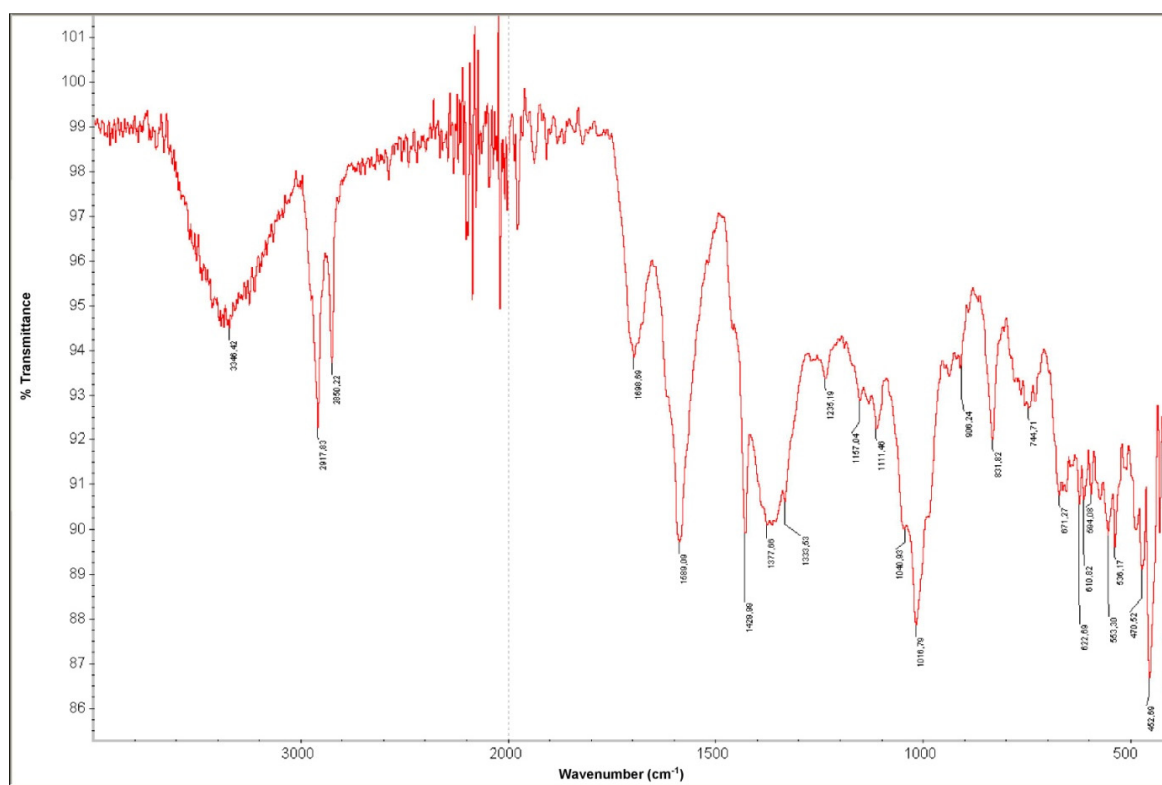


Figure S38. ATR-IR (film) spectrum of carbamidocyclophane S (7).

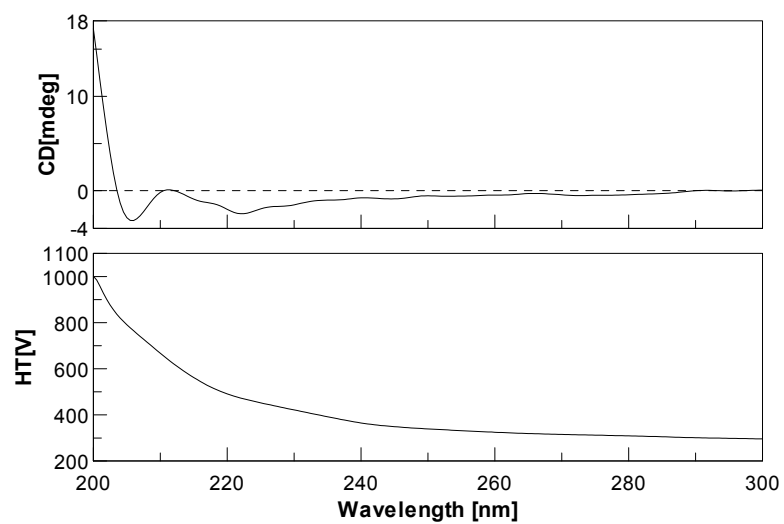


Figure S39. ECD spectrum of carbamidocyclophane S (7).

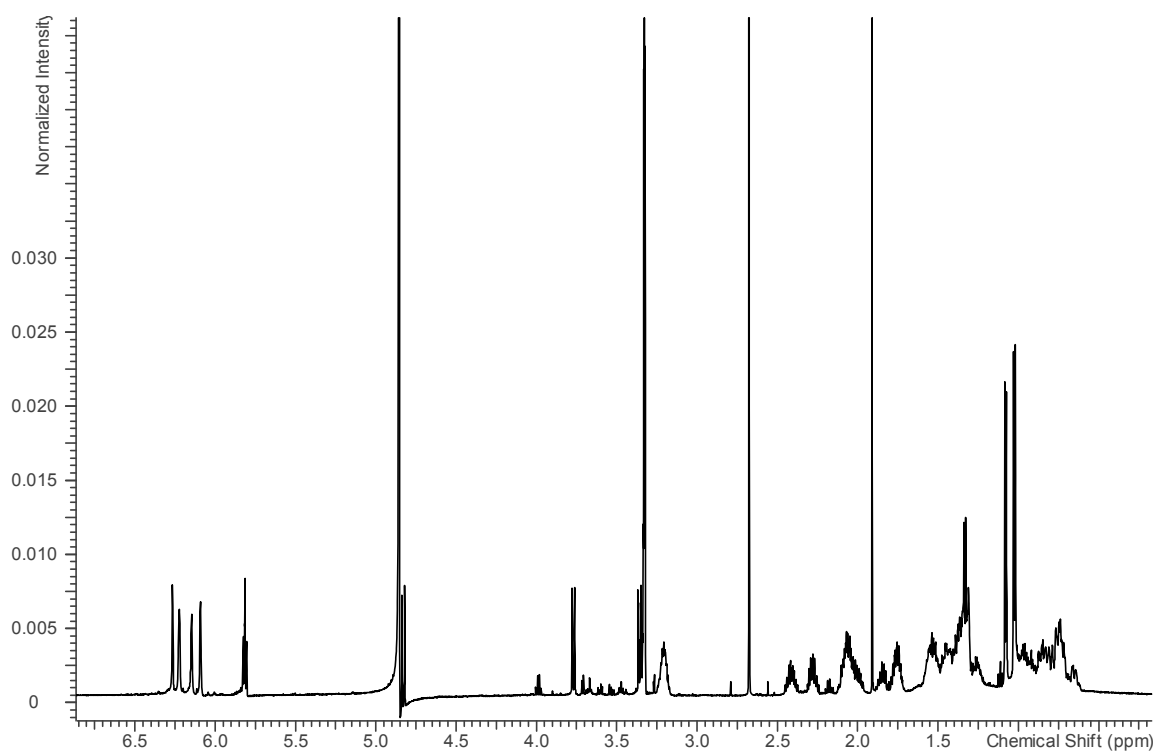


Figure S40. ^1H NMR spectrum (600 MHz, $\text{MeOH-}d_4$) of carbamidocyclophane T (8).

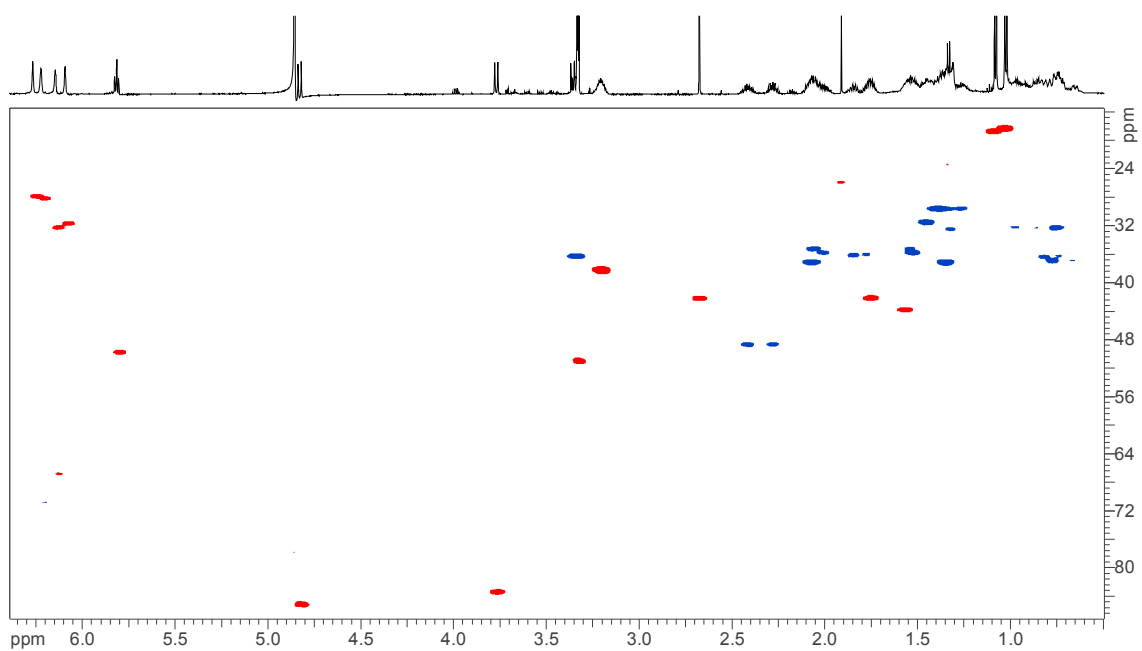


Figure S41. HMQC-DEPT spectrum (600 MHz, MeOH- d_4) of carbamidocyclophane T (**8**). Red signals are attributed to CH or CH₃ groups (positively phased) and blue signals to CH₂ groups (negatively phased).

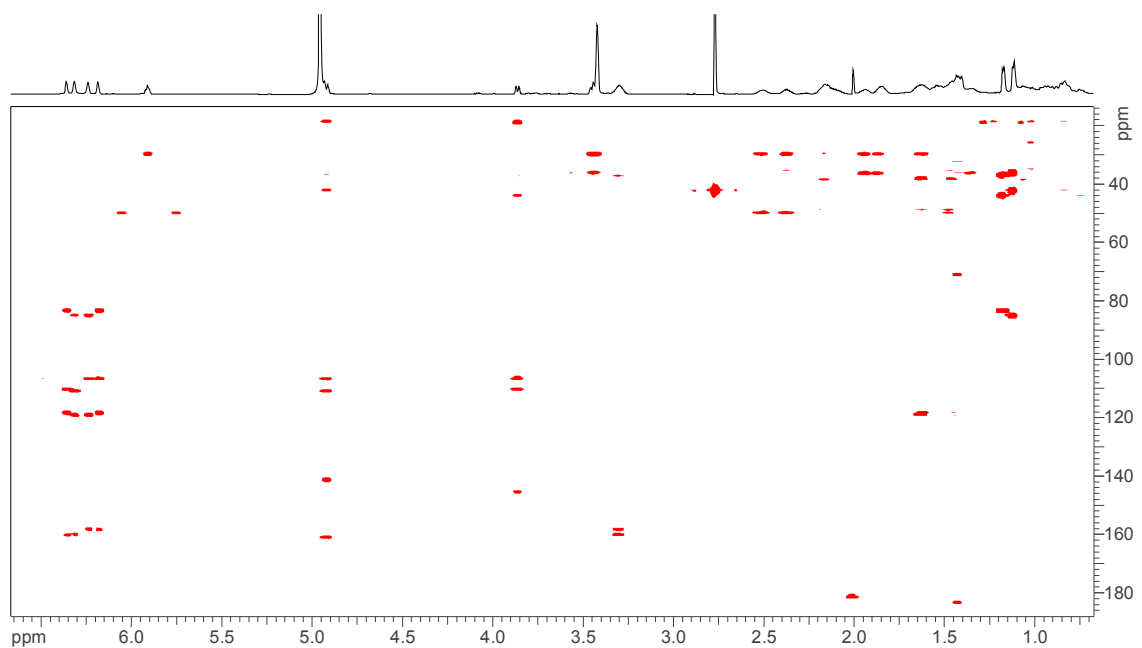


Figure S42. HMBC spectrum (600 MHz, MeOH- d_4) of carbamidocyclophane T (**8**).

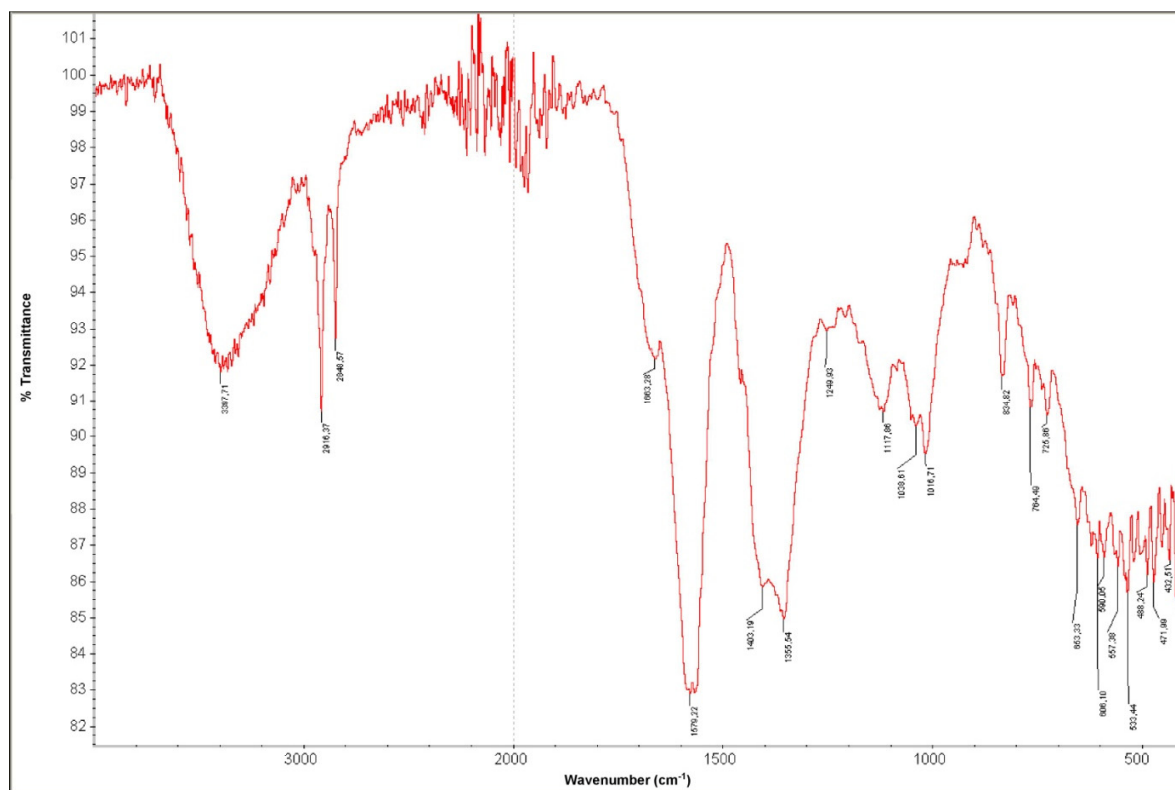


Figure S43. ATR-IR (film) spectrum of carbamidocyclophane T (8).

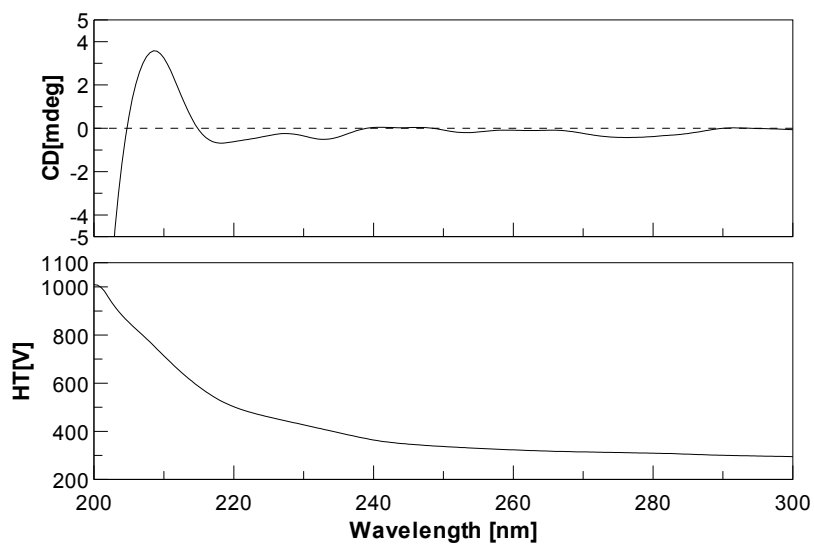


Figure S44. ECD spectrum of carbamidocyclophane T (8).

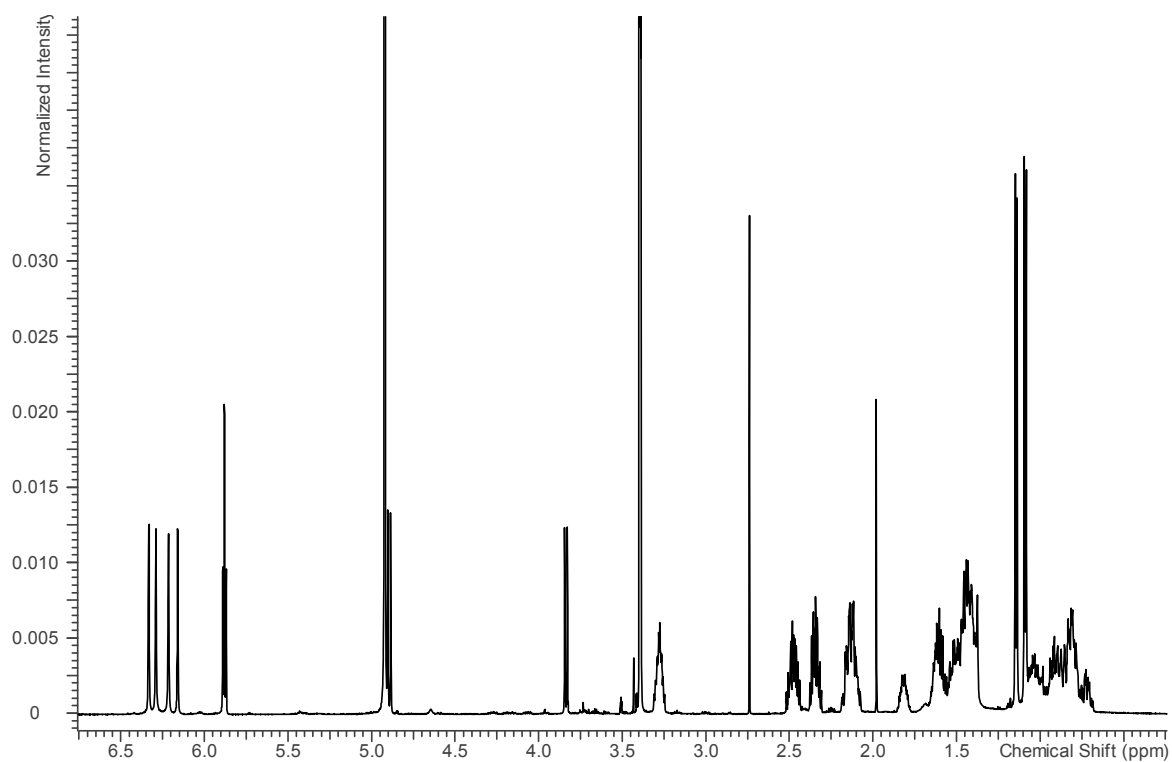


Figure S45. ^1H NMR spectrum (600 MHz, $\text{MeOH-}d_4$) of carbamidocyclophane U (9).

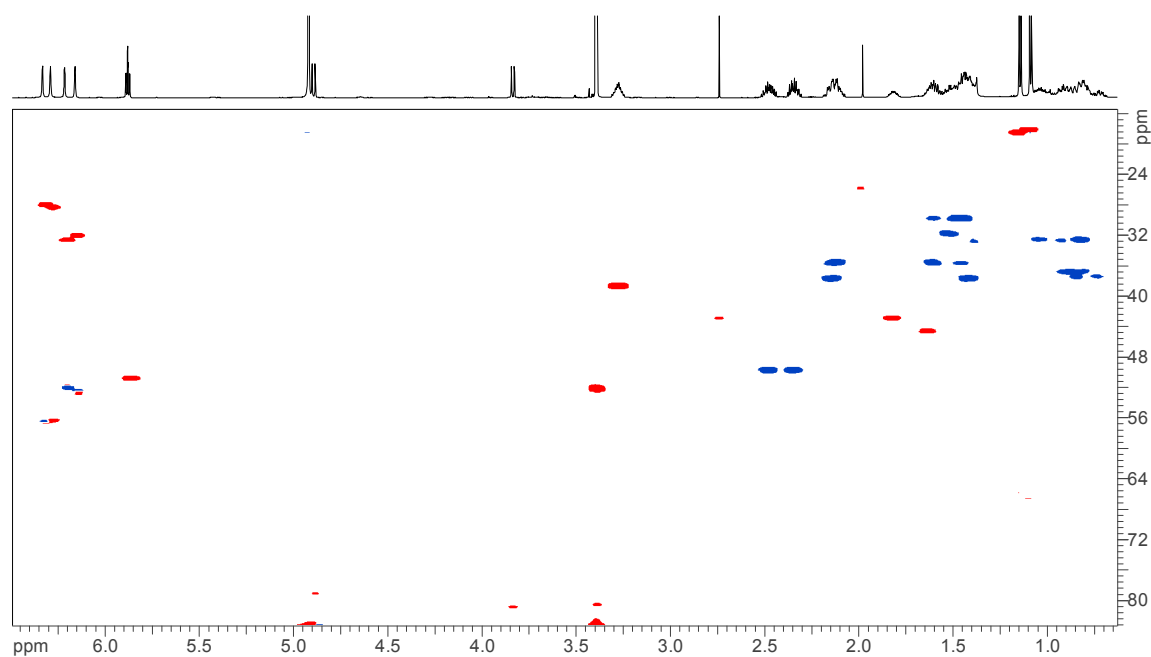


Figure S46. HMQC-DEPT spectrum (600 MHz, $\text{MeOH-}d_4$) of carbamidocyclophane U (9). Red signals are attributed to CH or CH_3 groups (positively phased) and blue signals to CH_2 groups (negatively phased).

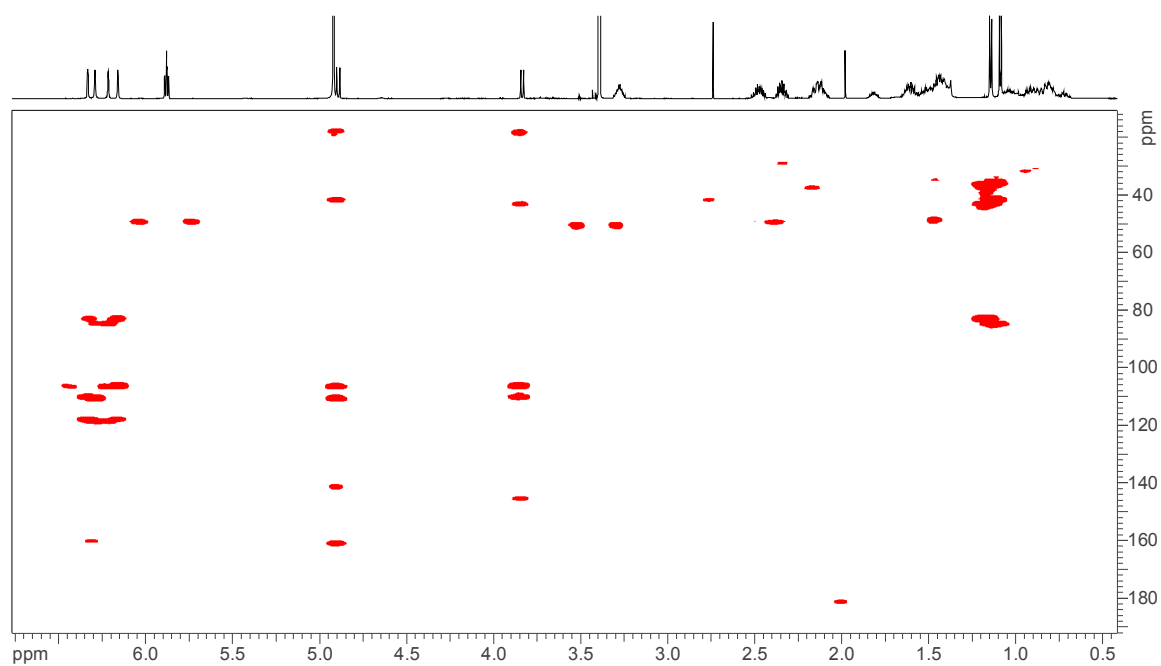


Figure S47. HMBC spectrum (600 MHz, MeOH-*d*₄) of carbamidocyclophane U (9).

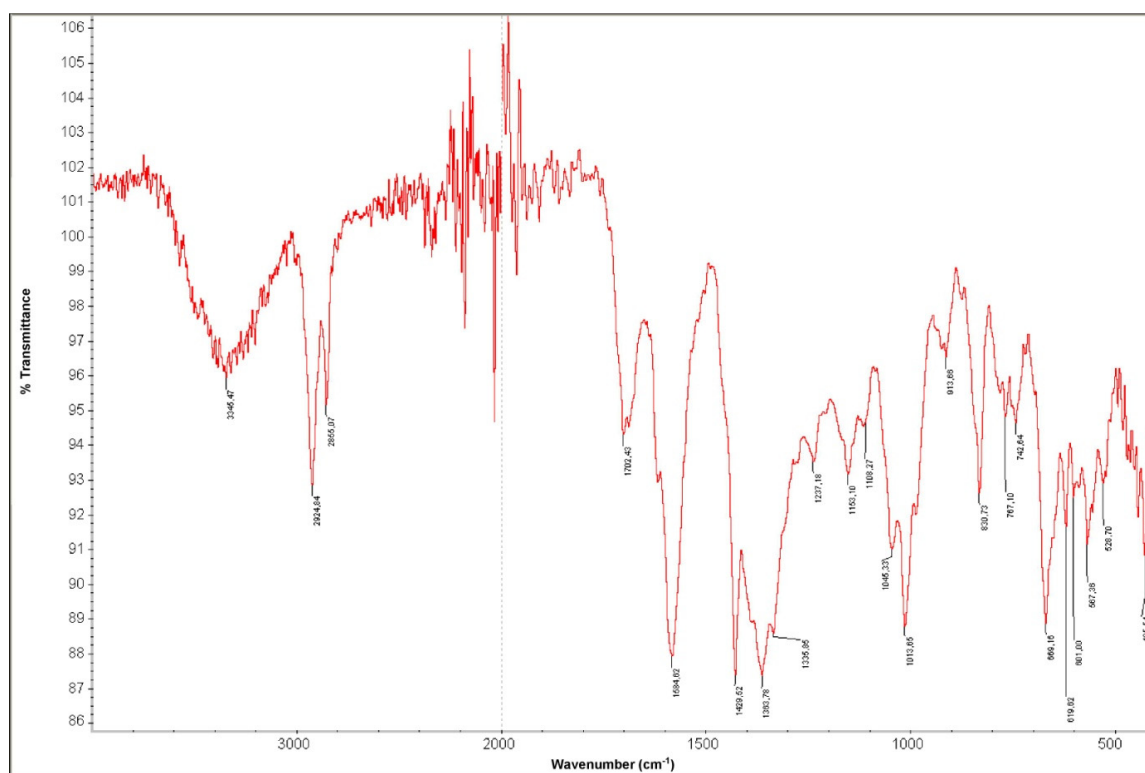


Figure S48. ATR-IR (film) spectrum of carbamidocyclophane U (9).

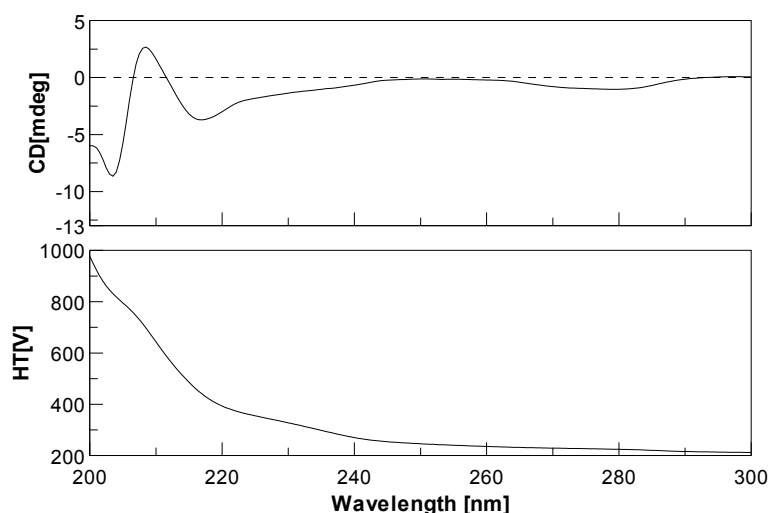


Figure S49. ECD spectrum of carbamidocyclophane U (9).

References

1. Falch, B.S.; König, G.M.; Wright, A.D.; Sticher, O.; Angerhofer, C.K.; Pezzuto, J.M.; Bachmann, H. Biological activities of cyanobacteria: evaluation of extracts and pure compounds. *Planta Med.* **1995**, *61*, 321–328.
2. Hughes, E.O.; Gorham, P.R.; Zehnder, A. Toxicity of a unialgal culture of *Microcystis aeruginosa*. *Can. J. Microbiol.* **1958**, *4*, 225–236.
3. Meffert, M.E. Cultivation and growth of two planktonic *Oscillatoria* spec. *Mitt. Int. Ver. Theor. Angew. Limnol.* **1971**, *19*, 189–205.
4. Pretsch, A.; Nagl, M.; Schwendinger, K.; Kreiseder, B.; Wiederstein, M.; Pretsch, D.; Genov, M.; Hollaus, R.; Zinssmeister, D.; Debbab, A.; et al. Antimicrobial and anti-inflammatory activities of endophytic fungi *Talaromyces wortmannii* extracts against acne-inducing bacteria. *PLoS ONE* **2014**, *9*, e97929.
5. Preisitsch, M.; Harmrolfs, K.; Pham, H.T.L.; Heiden, S.E.; Füssel, A.; Wiesner, C.; Pretsch, A.; Swiatecka-Hagenbruch, M.; Niedermeyer, T.H.J.; Müller, R., et al. Anti-MRSA-acting carbamidocyclophanes H-L from the Vietnamese cyanobacterium *Nostoc* sp. CAVN2. *J. Antibiot.* **2015**, *68*, 165–177.
6. Preisitsch, M.; Niedermeyer, T.H.J.; Heiden, S.E.; Neidhardt, I.; Kumpfmüller, J.; Wurster, M.; Harmrolfs, K.; Wiesner, C.; Enke, H.; Müller, R., et al. Cyliandrofridins A–C, linear cyliandrocylophane-related alkylresorcinols from the cyanobacterium *CyliandrospERMUM stagnale*. *J. Nat. Prod.* **2015**, doi:10.1021/acs.jnatprod.5b00768.